ELSEVIER

Palaeogeography, Palaeoclimatology, Palaeoecology 168 (2001) 39–74

PALAEO

www.elsevier.nl/locate/palaeo

Burrow-mediated carbonate dissolution in rudist biostromes (Aurisina, Italy): implications for taphonomy in tropical, shallow subtidal carbonate environments

D. Sanders*

Institute for Geology and Paleontology, University of Innsbruck, Innrain 52, A-6020 Innsbruck, Austria

Received 26 October 1999; received in revised form 19 September 2000; accepted for publication 11 October 2000

Abstract

In Upper Cretaceous rudist biostromes at Aurisina, Italy, marked taphonomic loss of radiolitids by burrow-mediated dissolution and mechanical disintegration illustrates the relation between synecology and early diagenesis in the fossilization of tropical shallow-water bioconstructions. The studied platform succession accumulated in a prevalently open lagoon with bioturbated carbonate sand, rudist thickets, bioclastic dunes, and areas with shelly lime ooze. Rudist biostromes consist of radiolitids and hippuritids, or of radiolitids only, and have an open, parautochthonous rudist fabric with a matrix of bioclastic, bioturbated wackestone. "Swirly" disorientation of bioclasts records early softground bioturbation. Later firmground burrows comprise an irregular network of tunnels and chambers filled with bioclastic packstone to grainstone. The size, geometry and sediment fill of the firmground burrows suggest that they were produced by crustaceans. Radiolitid preservation ranges from complete to relictic. Radiolitid relicts formed by (a) spalling and/or dissolution of the cellular boxwork ostracum of the attached valve, leaving "calcite-tubes" built by a distinct, thin ostracal shell layer, or (b) dissolution of the entire shell, leaving the sedimentary fills of the intertabular spaces of the attached valve as a diagnostic vestige, or (c) shell dissolution within the firm sediment, with subsequent filling of the biomould by bioclastic wackestone to packstone to grainstone. Loss of radiolitids produced a taphonomic bias towards rudists with non-cellular ostracum. Locally, taphonomic loss produced "ghost biostromes" composed nearly entirely of faint radiolitid relicts. Shell dissolution resulted from chemical gradients in the sediment within and near the burrows, and from enhanced microboring and microbial infestation. Dissolution of radiolitids was favoured by the combined effects of chemical instability of hypostracal aragonite and by the structure of the calcitic boxwork ostracum of thin-walled cells. Some biostromes are intercalated with, or are capped or overlain within a short vertical distance, by a hardly recognizable emersion surface, as a consequence of the shallow depth of biostrome accumulation. Taphonomic loss by dissolution is widespread in open, parautochthonous rudist fabrics, and confirms actuogeological results of other authors that bioturbation mediates carbonate dissolution also under shallow tropical waters supersaturated for calcium carbonate. The amount of carbonate dissolved upon burrowing of the biostrome matrix is hardly quantifiable but, by analogy to Recent carbonate environments, may have been large. Within bioconstructions, deep-tiered burrowing occurred at least since the Carboniferous. Taphonomic loss by dissolution thus may have been active in the fossilization of tropical shallow-water mounds and biostromes over much of Phanerozoic times.

Keywords: Cretaceous; Rudists; Bioturbation; Taphonomy; Diagenesis

* Fax: +43-512-507-2914.
E-mail address: diethard.g.sanders@uibk.ac.at (D. Sanders).

0031-0182/01/$ - see front matter
PII: S0031-0182(00)00249-2

1. Introduction

Geologists may infer that the rudist shells within a biostrome represent at least most of the rudists that originally lived at that site, or nearby. Taphonomic loss, if taken into account, is thought to result from physical agents, such as spill-away of shells during storms. Dissolution was not considered as a taphonomic agent. There seems little reason to assume dissolution, because the shallow neritic waters of the Cretaceous Tropics most probably were saturated to supersaturated with calcium carbonate (Woo et al., 1993; Barron and Moore, 1994), like Recent tropical shallow waters (e.g. Milliman, 1974; Bathurst, 1975). For Holocene siliciclastic shelves, however, many studies showed that shell dissolution within the soft sediment is a major factor in taphonomy (Peterson, 1976; Aller, 1978, 1982, 1983; Brett and Baird, 1986; Kidwell and Bosence, 1991). Except for a few restricted environments, shell production commonly is so high that, without dissolution, all the tropical to Arctic shelves were covered by a single, immense shell bed (e.g. Davies et al., 1989). Extensive dissolution of calcium carbonate was demonstrated also for Holocene tropical, shallow subtidal carbonate environments (Tudhope and Risk, 1985; Walter and Burton, 1990; Ku et al., 1999; see also May and Perkins, 1979; Walter and Morse, 1984). Dissolution of calcium carbonate proceeds within the soft to firm sediment and positively correlates with, and is directly related to, intensity and depth of burrowing (Peterson, 1976; Aller, 1978, 1982, 1983; Brett and Baird, 1986; Walter and Burton, 1990; Kidwell and Bosence, 1991; Ku et al., 1999), in particular to the deep-tiered, rapid burrowing by decapod crustaceans (e.g. Bromley, 1996). For mollusc faunas from the Late Cretaceous temperate chalk seas, Rasmussen (1971) and Koch and Sohl (1983) documented dissolution-induced taphonomic loss. For shallow subtidal carbonate rocks deposited in the Tropics, however, to date no documentation of dissolution and its possible impact on the taphonomy of bioconstructions (biostromes, skeletal mounds) exists.

How to produce evidence for something dissolved? For this purpose, rudists are ideal, because they abound in Cretaceous tropical platform successions, had quite different shell structures, and consist of both aragonite and calcite layers of different solubility and microstructure (cf. Walter, 1985). Furthermore, rudists commonly contain internal sediments of characteristic texture, shape and arrangement that allow for identification of relicts, even if all the shell has been dissolved (Sanders, 1999). Late Cretaceous rudists thrived in level-bottoms, biostromes and gentle mounds (Kauffman and Johnson, 1988; Ross and Skelton, 1993; Gili et al., 1995). Rudist accumulations thus share characteristics with shell beds to skeletal mounds.

At Aurisina in northern Italy (Fig. 1), Upper Cretaceous platform limestones are quarried by cutting blocks a few metres in size with steel wire. This method yields quarry walls that excellently expose the limestones. Moreover, numerous cut blocks and huge slabs stored aside each quarry allow for a close-up, three-dimensional study of lithologies and fossils with a detail and on a scale that is rarely, if ever, possible in field geological investigations. The study of the limestones at Aurisina triggered recognition of rudist taphonomic phenomena in less well-exposed rudist formations in Austria, Italy, Spain and Hungary. In a previous paper, the construction of the radiolitid shell and its styles of disintegration were described (Sanders, 1999). The present paper documents (1) taphonomic

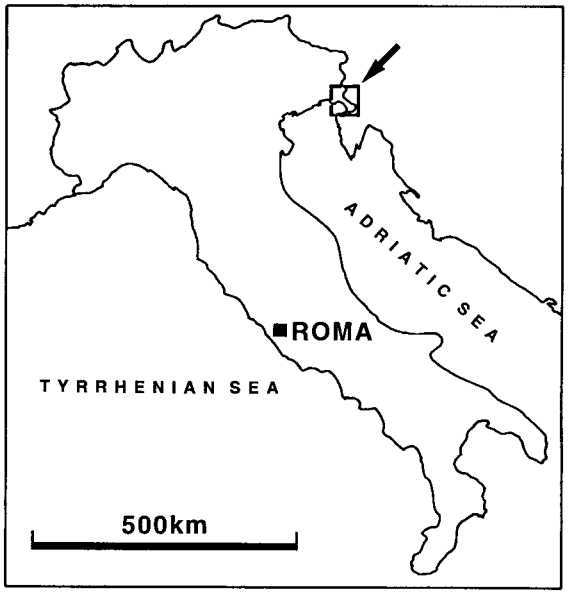

Fig. 1. Position of the area of Aurisina and Trieste (heavy black quadrangle labelled by arrow) in Italy.

loss in rudist biostromes as a result of dissolution mediated by softground to firmground burrowing, and (2) the relation of emersion surfaces to preservation of rudist biostromes. The results are relevant for the palaeoecologic and sedimentologic interpretation of Phanerozoic tropical skeletal accumulations.

2. Geological setting

The Friuli carbonate platforms were situated at the northwestern corners of the Adriatic and Dinaric isolated carbonate platforms, respectively (Fig. 2; Cati et al., 1987), that extended from 25°N down to 15°N Late Cretaceous latitude (Philip et al., 1993). These platforms were part of the peri-Adriatic archipelago of isolated carbonate shelves that came into existence upon Jurassic rift-induced segmentation of the Hauptdolomit megabank (Bernoulli and Jenkyns, 1974). The Friuli platforms possibly were separated by a Jurassic to Late Cretaceous seaway (Friuli basin; Fig. 2) of poorly constrained width and extent (D. Sartorio, 1999, personal

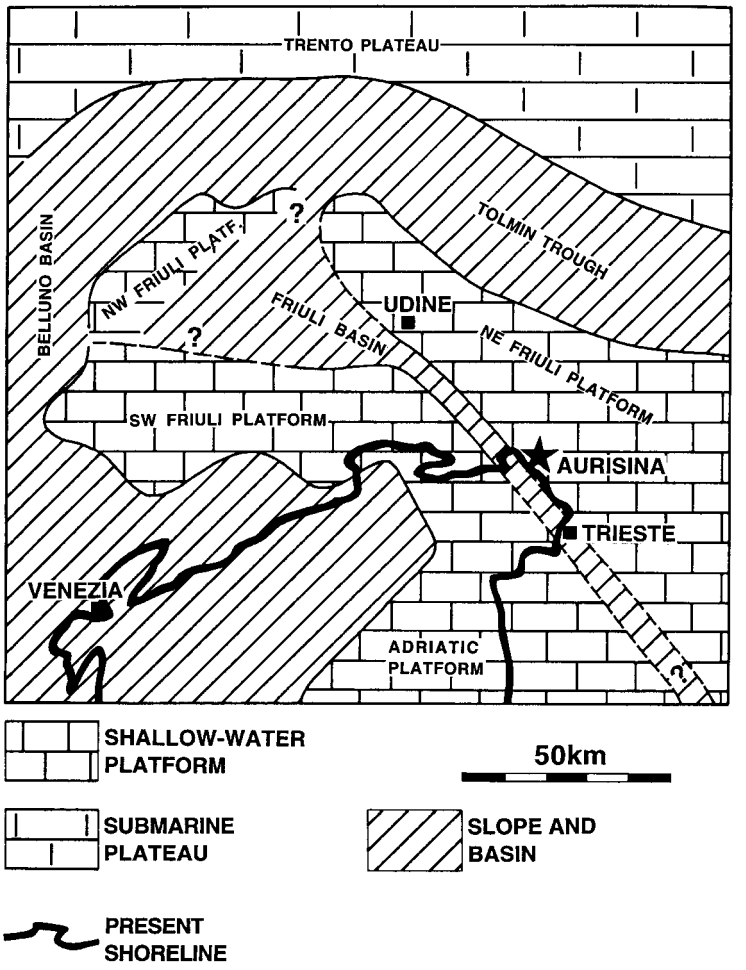

Fig. 2. Late Cretaceous palaeogeography of the Friuli carbonate platforms and environs (after Cati et al., 1987). A former seaway, the Friuli basin, separated three Friuli platforms. The width and southward continuation of the Friuli basin are poorly constrained. During the Late Cretaceous, the area of Aurisina probably was situated near the margin of the NE Friuli platform which, in turn, represented the northwestern corner of the larger Dinaric platform.

comm.). During the Late Cretaceous the area of Aurisina may have been situated up to more than 10 km behind the southern margin of the Northeastern Friuli platform (Fig. 2; compare Cati et al., 1987, Figs. 7 and 8). The outcrop intersection subparallel to depositional strike does not allow for a closer estimate (see Fig. 3). During the latest Cretaceous to Palaeocene, the Friuli platforms were subaerially exposed. Upon Late Maastrichtian to Eocene transgression, shallow-water platform deposition resumed. Subsequently, the platforms entered the Adriatic foredeep, were covered by Eocene flysch, and were folded and thrusted with top southwest (Fig. 3) (Massari et al., 1986; Cucchi et al., 1987; Sartorio et al., 1997).

The Cretaceous between Aurisina and Trieste records a development from an Aptian to Cenomanian restricted inner platform to a Campanian to Maastrichtian open, shallow subtidal environment (Cucchi et al., 1987). The investigated succession is situated within the Borgo Grotta Gigante Member (Turonian to Maastrichtian) that is up to 1000 m thick (Fig. 3) (Cucchi et al., 1987). The Borgo Grotta Gigante Member is dominated by rudist-clastic packstones to grainstones with intercalated rudist biostromes. Locally, intervals of wackestones, lime mudstones with desiccation cracks, black pebble breccias and characean limestone record protected marine-subtidal to supratidal to lacustrine environments (Cucchi et al., 1987; Tentor et al., 1994). In the Santonian to Campanian part, a megabreccia is overlain by fossiliferous black shales that probably were deposited in a restricted intra-shelf basin (Cucchi et al., 1987; Tarlao et al., 1993; Tentor et al., 1994).

At Aurisina, the largest quarry in the Borgo Grotta Gigante Member is Cava Romana that consists of several active and inactive pits down to about 40 m in depth and a few hundreds of metres in width. At Cava Romana, a Campanian age is indicated by the assemblage of *Kuehnia* Milovanovic, *Katzeria* Sliskovic, *Rajka* (*Biradiolites*) d'Orbigny, *Pseudopolyconites* Milovanovic, *Radiolites* ("*Gorjanovicia*") Lamarck and *Hippurites nabresinensis* Futterer (Cucchi et al., 1987; Caffau and Plenicar, 1990; Sribar and Plenicar, 1990; Cestari and Sartorio, 1995). Another quarry investigated for rudist taphonomy is Cava Cortese near San Pelagio, close to Aurisina. Cava Cortese is about 10 m in height and several tens of metres wide, and is situated in the Turonian to ?Santonian part of the Borgo Grotta Gigante Member. Because of the poor preservation of the rudists, no precise age can be provided.

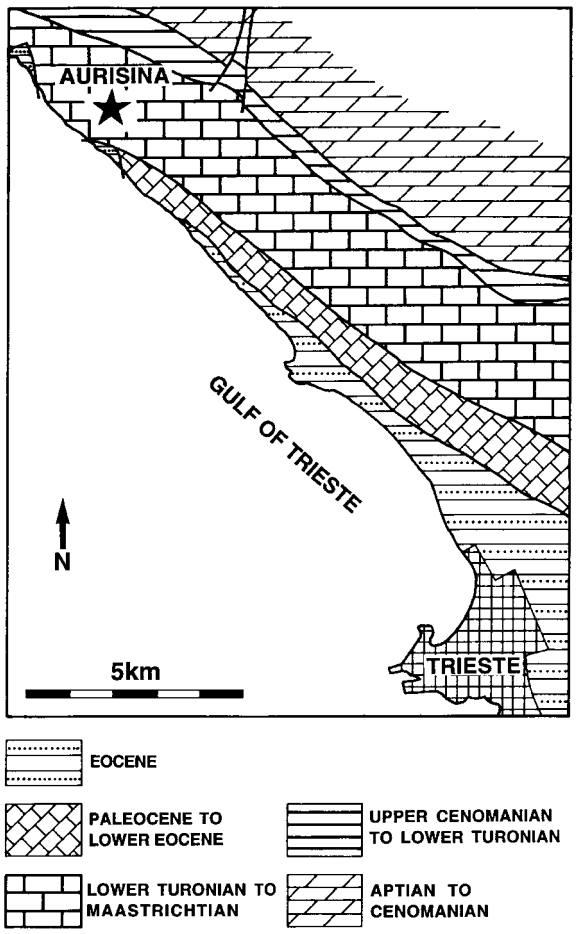

Fig. 3. Geological map of the area between Aurisina and Trieste (simplified from Cucchi et al., 1987). Aptian to Cenomanian restricted inner carbonate platform deposits are followed up-section by an Upper Cenomanian to Lower Turonian succession that records an intermittent deepening, down to deep open lagoonal conditions. Above, a succession about 1000 m thick of limestones of Early Turonian to Maastrichtian age is present (Borgo Grotta Gigante Member of Trieste Karst Limestone Formation; Cucchi et al., 1987). The Borgo Grotta Gigante Member is unconformably overlain by Palaeocene to Lower Eocene shallow-water limestones that record an overall deepening. The upper part of the exposed succession consists of Eocene flysch.

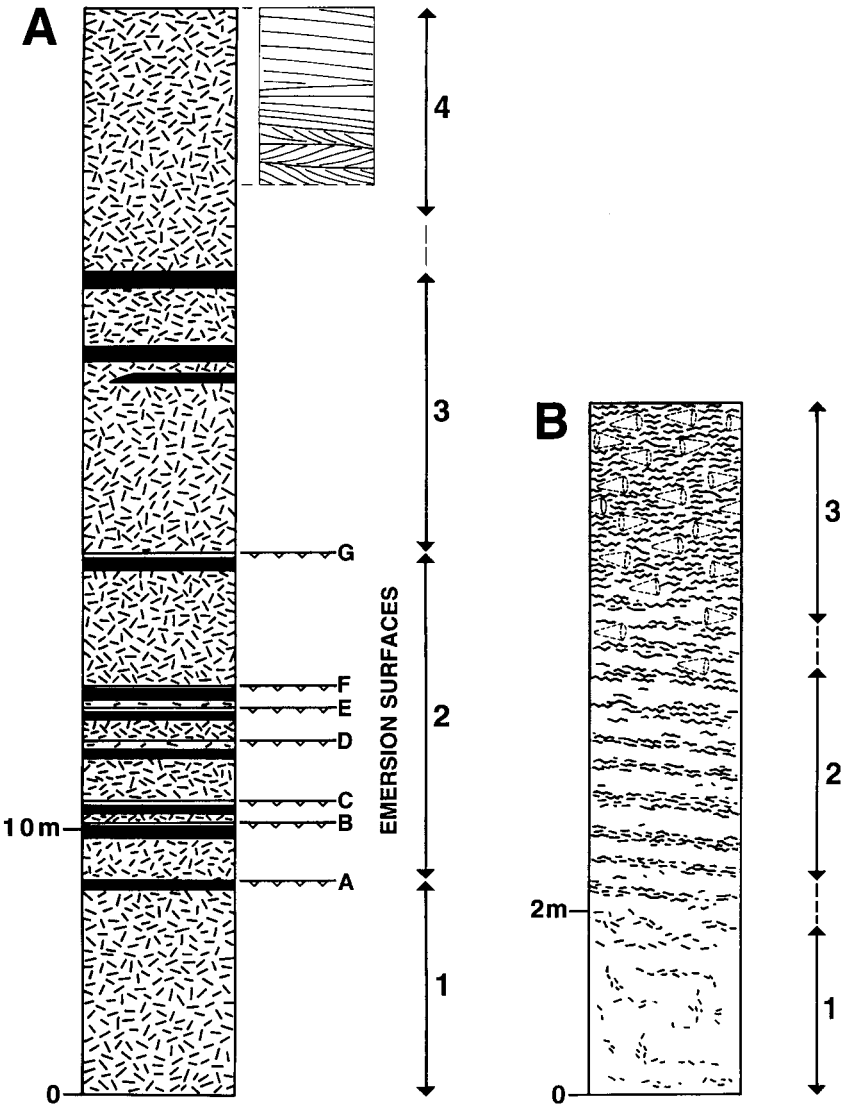

Fig. 4. (A) Succession in Cava Romana, Aurisina. Interval 1 is subparallel-bedded and consists mainly of bioclastic limestones. It is topped by a radiolitid biostrome that, in turn, is capped by emersion surface A. Interval 2 consists of interlayered bioclastic limestones and rudist biostromes, and is intercalated with emersion surfaces B to G. Interval 3 is dominated by bioclastic limestones, and contains three biostromes in its upper part. Emersion surfaces could not be identified with certainty. Interval 4 consists of cross-stratified bioclastic grainstone. (B) Succession in Cava Cortese near San Pelagio/Aurisina. Interval 1 consists of bioclastic wackestone to packstone to, locally, floatstone. Up-section, interval 1 grades into interval 2, a package of bioclastic wackestone to packstone with intercalated layers of radiolitid-clastic floatstone. The topmost interval 3 consists of radiolitid-clastic floatstone to rudstone. In the floatstone to rudstone, abundant relicitic structures (dashed symbols) of radiolitids are present (see text).

3. Methods

Since the wall of the main pit of Cava Romana is inaccessible, the section shown in Fig. 4A was constructed by inspecting the wall with a binocular, and estimating the vertical distances by comparison to objects of fairly precise size. In the quarry wall, the biostromes are well visible. Some biostromes show a characteristic fabric, thickness, preservation and vertical association with other features, such as

emersion surfaces. These biostromes could be identified in the numerous blocks and slabs stored aside the quarry. For other, less characteristic biostromes within the quarry wall, no clear-cut relation could be established to similar biostromes in blocks and slabs aside the quarry. Because this study deals mainly with styles of rudist preservation, the drawback of the relatively imprecise section of Cava Romana was compensated by the possibility for detailed close-up study of rudist biostromes and their vertically associated limestones.

To deduce the relation of rudist taphonomy to stratigraphic development and facies dynamics, the diagenesis of the limestones was studied. The quantitative determination of the calcite and dolomite content of the samples was made with the program "Diffrac Plus" coupled to a Siemens D-500 X-ray diffractometer. Cathodoluminescence microscopy was performed with a "Cold cathodoluminescence Model 8200 MK II". The vacuum was set at <0.1 Torr at approximately 20 V. Acceleration voltage was adjusted between 15 and 20 kV, with a gun current of 500–600 mA. Samples for stable isotopes of oxygen and carbon, and for determination of trace element contents were taken with a dental drill from rock slabs. For bulk rock samples, an area of about 1–2 cm^2 was drilled. Isotope samples from radiolitids were taken from ostracal, calcitic shell parts that are composed of non-cellular calcite. The stable isotopes were measured at a Finnigan MAT-Deltaplus isotope ratio mass spectrometer. Carbon dioxide was extracted by reaction of the samples with 10.3% phosphoric acid at 70°C (McCrea, 1950). The internal CO_2-reference gas was calibrated against the NBS-18 international calcite standard (Abart et al., 1998).

For determination of Fe, Mn and Sr, each sample was dissolved in 65% nitric acid and subsequently diluted with Aqua bidest up to 6 ml. The contents of Fe, Mn and Sr were measured with a Philips PU 7000 ICP spectrometer. Iron was measured at the 259.94 nm wave length, manganese at 257.61 nm and strontium at 421.552 nm wave length.

4. Sedimentary facies

4.1. Rudist-clastic grainstone to packstone

At Cava Romana, the Borgo Grotta Gigante Member is dominated by cream to light-grey coloured, very poorly to well-sorted, coarse to fine sand rudist-clastic grainstones to bioturbated packstones (Fig. 4A). The grainstones are bioturbated, or are cross-laminated. Intervals of cross-laminated grainstone typically consist of stacked, bidirectionally inclined sets each 10–30 cm thick of oblique-tangential laminae. These stacked laminasets are locally intercalated with sets up to about 1.5 m thick of unidirectionally inclined, oblique-tangential to sigmoid-tangential beds that internally are laminated parallel to bedding. The bioclastic sand consists of both angular, non-micritized and well-rounded rudist fragments with a micrite rim and, subordinately, of variable amounts of benthic foraminifera (miliolids, textulariines, small rotaliaceans), fragments of echinoids, red algae, skeletal sponges, serpulid tubes, calcareous green algae, alcyonarian sclerites, microgastropods, bryozoan fronds, and rounded plasticlasts a few millimetres to about 1 cm in size of microbioclastic packstone. The plasticlasts locally make up to a few percent of the limestones. In the cross-laminated/cross-stratified grainstones, locally subvertical burrows and, more rarely, irregular networks of *Thalassinoides* about 2–5 cm in diameter are present. The burrows are filled either with microbioclastic packstone or, more commonly, with medium grey bioclastic packstone to grainstone that is of closely similar composition than the host limestone. Locally, the host limestone adjacent to burrows has been disintegrated into rounded clasts up to several centimetres in size.

4.1.1. Interpretation

The rudist-clastic grainstones to packstones were deposited in an open, shallow subtidal environment of moderate to high water energy. The intervals of cross-laminated/cross-stratified grainstones were deposited from subaqueous dunes. The plasticlasts of microbioclastic packstone may have been eroded during high-energy events from muddy bottoms. This, however, seems improbable because of the uniform composition of the clasts and the absence of fossils of quiet, shallow subtidal areas (e.g. miliolids, lituolaceans, calcareous green algae). Alternatively, the plasticlasts may be sediment pellets produced by crustacean burrow excavation, or represent

disaggregated polychaete biodeposits (cf. Farrow, 1971; Braithwaite and Talbot, 1972).

The burrows in the grainstones were excavated when the sediment was firm, as indicated by the local disintegration of matrix adjacent to the burrows into rounded clasts. In Holocene tropical carbonate environments, thalassinidean crustaceans are both the most common and most effective deep-tiered burrowers (e.g. Griffis and Suchanek, 1991; Bromley, 1996). These crustaceans excavate extensive open burrow networks down to several metres in depth. In the deeper levels, because of mechanical compaction the substrate provides a firmground (Ekdale, 1985; Bromley, 1996). Similar burrows, but much more common and better developed, are present in intervals of rudist limestone (see below).

4.2. Rudist limestone

At Cava Romana, sheets a few decimetres to about 1.5 m thick of rudist bafflestone to floatstone are present (Fig. 4A). The lowest sheet of rudist limestone (black interval below surface A in Fig. 4A) is about 30 cm thick, and consists of *Radiolites* bafflestone with a matrix of rudist-clastic wackestone to lime mudstone (Fig. 5). The overlying intervals of rudist limestone, by contrast, are bafflestones to floatstones with several genera of radiolitids and, subordinately,

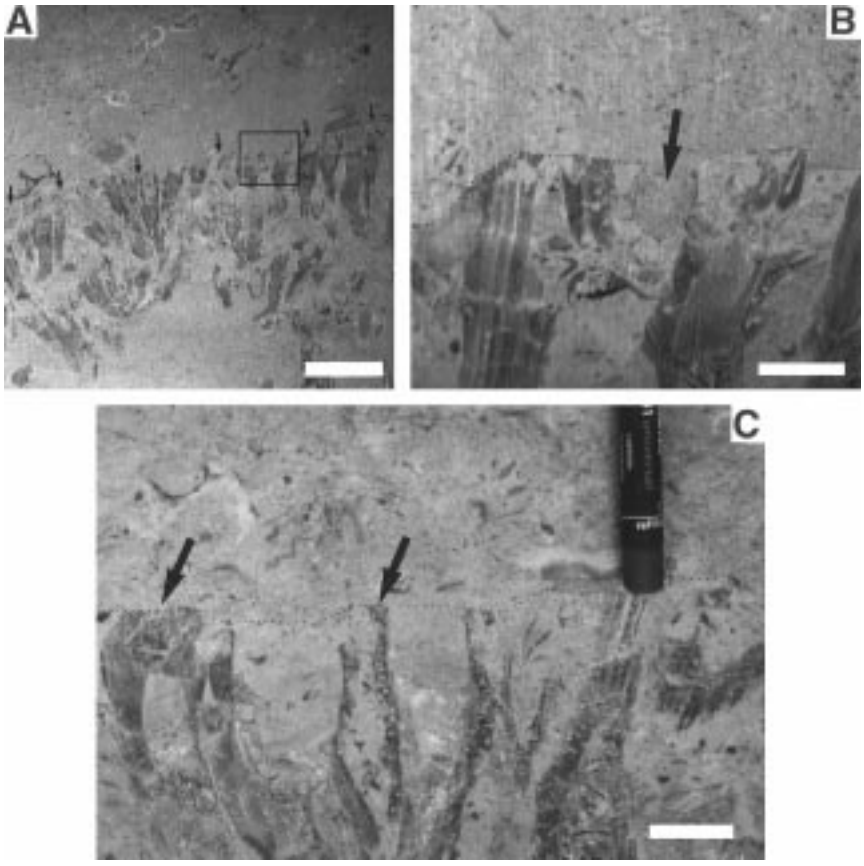

Fig. 5. (A) *Radiolites* thicket, capped by a hardground (indicated by arrows). The thicket bears a matrix of rudist-clastic wackestone, and is sharply overlain along the hardground by bioturbated, fine-grained bioclastic packstone with floating, large rudist fragments. Rectangle marks area shown in B. Scale bar: 10 cm. (B) Along the hardground (fine stipples), the radiolitid shells are truncated. The hardground shows a small embayment (arrow) that is similar to corrosion pits produced by boring bivalves. Scale bar: 2 cm. (C) Detail from hardground shown in A. Along the hardground (fine stipples), the radiolitid shells are truncated (arrows). Scale bar: 2 cm.

hippuritids. Among the radiolitids *Radiolites*, *Biradiolites*, *Bournonia* Fischer, "*Gorjanovicia*", *Rajka* (*Biradiolites*) and *Katzeria* are common. The hippuritid fauna is dominated by *Hippurites nabresinensis* and by *Vaccinites* spp. (Cucchi et al., 1987; Caffau and Plenicar, 1990). Most rudists are isolated and embedded in a disoriented position, but some isolated specimens and, locally, small clusters are preserved in situ; the upper valve most commonly is absent. Locally, rudists and rudist fragments are encrusted by coralline algae, calcisponges, ruperti-nines and microbialites, but overall encrustation is scarce. Crushed rudist shells indicate mechanical compaction.

The matrix is a bioturbated, very poorly sorted rudist-clastic wackestone to packstone with miliolids and lituolaceans, and with fragments of echinoids, bryozoans and calcareous green algae. Bioturbation is indicated by "swirly" arrangement of elongate and platy bioclasts. The bioturbated matrix, in turn, is riddled with faint burrows filled with bioclastic pack-stone to wackestone closely similar in composition and colour to the matrix (Fig. 6). The boundary between matrix and burrow fills can only locally be

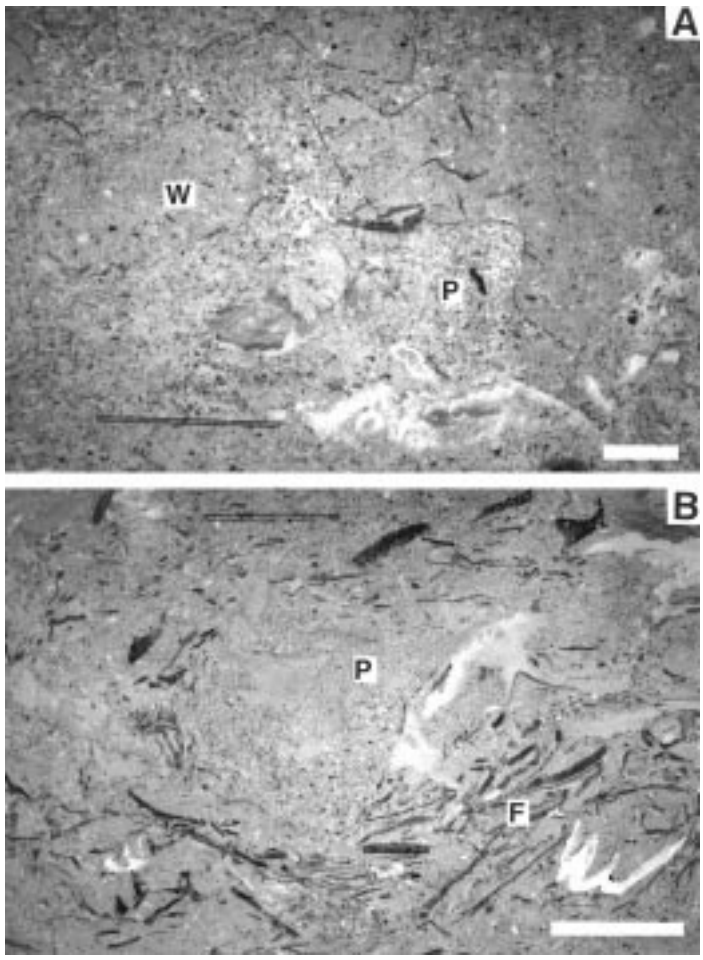

Fig. 6. Bioturbated matrix of rudist biostromes. (A) Bioturbation distinguished by textural difference between pods of rudist-clastic wackestone (w; outlined with pencil) and rudist-clastic packstone (p). Scale bar: 2 cm. (B) Bioturbation visible by disorientation of coarse rudist fragments within a rudist-clastic floatstone (f), and by a textural difference between the floatstone and a better-sorted bioclastic packstone (p). Scale bar: 5 cm.

identified, and is typically gradual. Both the bioturbated matrix and the faint burrows are cross-cut by another burrow generation. These latter burrows are subvertical tubes to irregularly shaped networks of tubes interspersed with wider chambers. The tubes typically are 2–6 cm in diameter, whereas the chambers may be up to 20 cm wide (Figs. 7 and 8). These burrows most commonly are filled with a medium to dark grey, poorly to moderately sorted, medium to coarse sand rudist-clastic packstone to grainstone. Because of their darker colour, these burrow fills are well visible from distance; they are present over the entire exposed length of the intervals of rudist limestone. On the upper surface of blocks cut subparallel to bedding, subcircular patches about 2–6 cm in diameter filled with bioclastic limestone are present, and are spaced about 10 cm to a few decimetres apart. Where these patches are situated along the intersection of two block surfaces, they are connected with the burrow network on the surfaces cut vertical to bedding. On the latter surfaces, no preferred orientation of the burrow network could be discerned.

On the surfaces cut perpendicular to bedding, straight tunnels may extend over several decimetres in length. More commonly, depending on the intersection of tunnels with the cut surface, it is riddled with subcircular to elliptical to tunnel-shaped burrows (Figs. 7 and 8). Locally, the lower part of the burrow chambers is filled with faintly geopetally laminated lime mudstone to rudist-clastic wackestone of identical colour to the host limestone; the upper part of these chambers again is typically filled with the darker grey bioclastic calcarenites. In thin-section, the boundary between the fill of the burrow network and the host sediment is either sharp or gradual over a distance of 1–2 mm. No burrow linings were observed. As for the grainstones described above, the host limestone adjacent to burrows locally is disintegrated into rounded clasts.

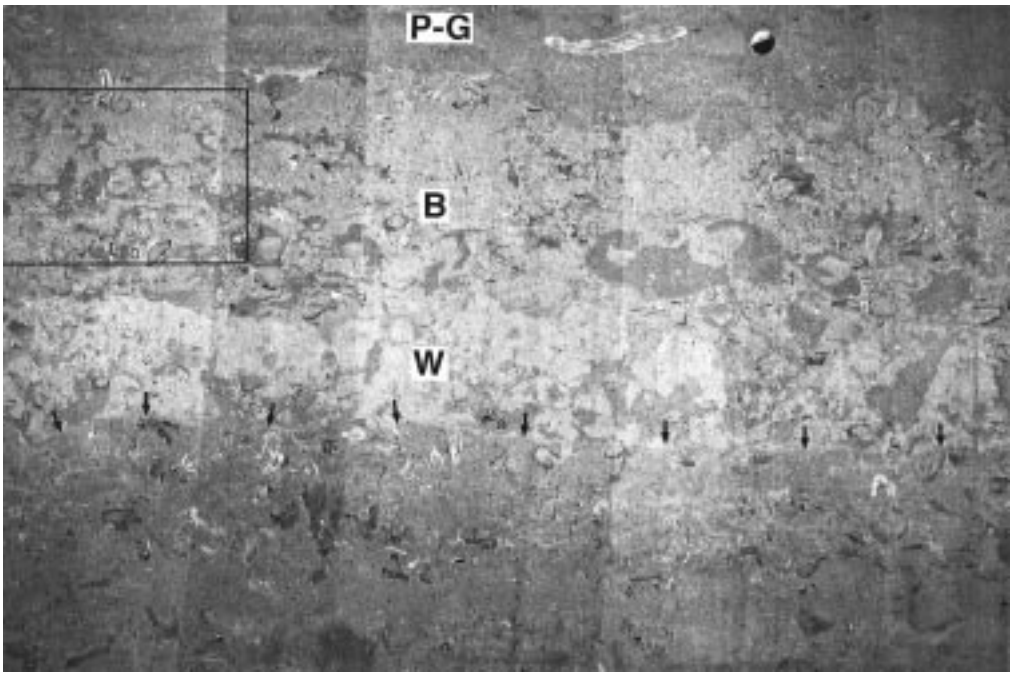

Fig. 7. 1.4 m wide view of a cut block. In its lower part, the block consists of an interval with parautochthonous, open rudist fabric of radiolitids and, subordinately, of hippuritids. This interval is topped by a hardground (indicated by small arrows) with a slightly irregular small-scale relief. Above, an interval of poorly sorted rudist-clastic wackestone (W) with a few disoriented rudists is overlain by a biostrome with an open, parautochthonous fabric (B). Intervals W and B are riddled by a network of tunnels and chambers filled with bioclastic packstone to grainstone (slightly darker grey areas). Interval B, in turn, is overlain by coarse sand bioclastic packstone to grainstone (P–G). The boundary between the biostrome and the overlying bioclastic limestones is irregular due to bioturbation. Rectangle indicates area of Fig. 8.

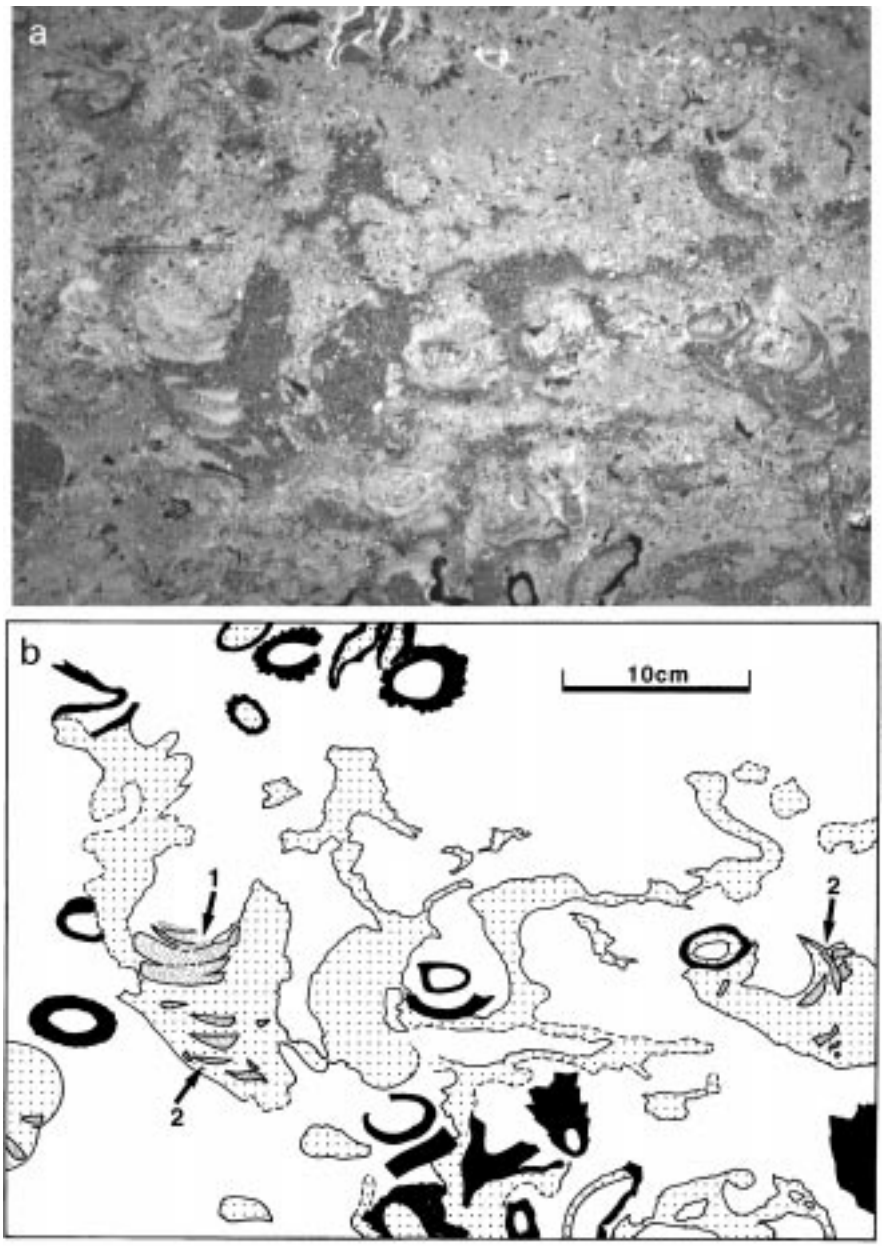

Fig. 8. Photograph and line-drawing of a biostrome, cut perpendicular to bedding. Rudist shells and large shell fragments shown black. The matrix (white) of the biostrome is a bioturbated, rudist-clastic wackestone to packstone, and is riddled with burrows that are filled with coarse sand rudist-clastic packstone to grainstone (stipples). The boundary between matrix and burrow fill mostly is well defined, but locally is gradual (dashed) both with respect to rock colour and sediment texture. Crescent-shaped components (fine stipples; arrows 1, 2) of light grey mudstone to fine-sand bioclastic wackestone locally float within the burrow fill.

4.2.1. Interpretation

The sheets of rudist limestone were deposited from biostromes that accumulated under overall moderate to low water energy. Because most rudists are not in situ and are supported by matrix, the biostromes show an open, parautochthonous rudist fabric (cf. Sanders and Pons, 1999). The cross-cutting relations of the different types of burrows are mainly related to increasing substrate coherence. Although resolved as "generations" of bioturbation, during biostrome accumulation burrowing may have proceeded nearly continuously. The first burrow generation was produced in a softground; the second generation records a slightly cohesive substrate that allowed for local burrow preservation. For the third generation, the good preservation of the burrow network, the distinct fill, the absence of burrow linings, and the observation that the adjacent host limestone locally disintegrated into clasts indicate that these burrows were excavated when the sediment was firm, resulting in an open burrow network. With respect to their diameter, overall size, geometry and fill, the third-phase burrows are closely similar to Holocene decapod burrow networks (e.g. Shinn, 1968; Braithwaite and Talbot, 1972; Griffis and Suchanek, 1991; Tedesco and Wanless, 1991; Bromley, 1996). The geopetally laminated lime mudstone to rudist-clastic wackestone that is locally present in the lower part of the burrow chambers was either swept in during episodic high-energy events (cf. Wanless et al., 1988; Tedesco and Wanless, 1991), and/or rained down from unstable portions of the chamber wall (Shinn, 1968).

4.3. Rudist-clastic floatstones to rudstones

In the main pit of Cava Romana, intervals up to about 3 dm thick of rudist-clastic rudstone locally associated with parallel-laminated rudist-clastic grainstones to packstones make up a small portion of the succession. At Cava Cortese, the upper part of the succession (interval 3 in Fig. 4B) consists of floatstones to rudstones composed of platy, calcitic radiolitid fragments, a few fragments from the cellular ostracum of the attached radiolitid valve and, locally, a few small disoriented radiolitids with an ostracum of non-cellular calcite. The platy, calcitic fragments were derived from disintegration of the ostracal portion of the free valve, and from packages of merged radial funnel plates of the lower radiolitid valve (cf. Sanders, 1999). Weathered surfaces of these floatstones to rudstones exhibit mainly the calcitic fragments (Fig. 9A). In cut blocks and slabs of the floatstones to rudstones abundant "white spots" some centimetres in size are present (dashed symbols in Fig. 4B; see Fig. 9B). Bioturbation is recorded by "swirly" arrangement of the platy calcitic fragments, and by burrow mottles of wackestone to packstone texture. Crushing of many of the platy radiolitid fragments and, locally, a schlieren-like fabric composed of platy fragments and the "white spots" indicate substantial mechanical compaction.

4.3.1. Interpretation

At Cava Romana, the few intervals of rudist rudstone probably formed by fragmentation of rudists during high-energy events. At Cava Cortese, the described floatstones to rudstones represent a characteristic lithology in association with radiolitid biostromes. Because the platy, thin fragments had a large surface relative to their weight, and because the limestones consist nearly exclusively of these fragments, these floatstones probably formed by transport and accumulation of the platy fragments from feeble currents (Amico, 1978; Sanders, 1999). The white spots up to some centimetres in size are interpreted as the sedimentary fill of radiolitids that were dissolved at a very early stage of diagenesis (see chapter 7 for description).

4.4. Bioclastic wackestone to packstone

Bioturbated wackestone to packstone dominated by more-or-less micritized rudist fragments builds the larger part of the succession in Cava Cortese (intervals 1 and 2 in Fig. 4B). Aside rudist fragments, these limestones contain miliolids, lituolaceans, fragments of echinoids and calcareous green algae, cryptmicrobial lumps, and peloids. In the succession of Cava Romana, intervals up to a few decimetres thick of wackestones of similar composition are quite rare.

4.4.1. Interpretation

The wackestones to packstones accumulated in open, shallow subtidal environments of moderate to

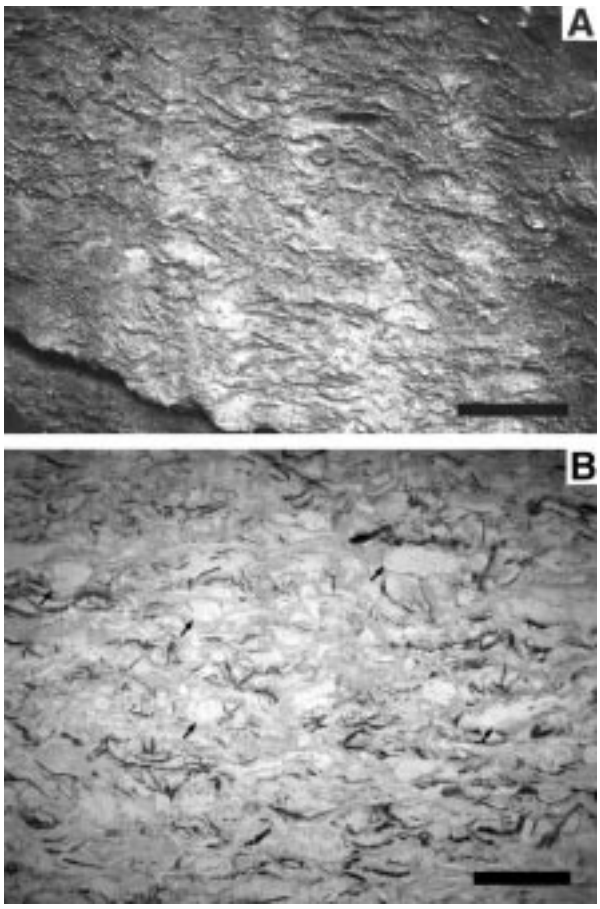

Fig. 9. (A) Limestone weathered under soil and exhumed. Abundant platy fragments from the massive, calcitic parts of radiolitids (mainly fragments of the ostracum of the upper valve) are visible. Scale bar: 10 cm. (B) Slab cut perpendicular to bedding from the same limestone. The only shells or shell fragments preserved are of primary calcitic composition. Aside from the numerous calcitic radiolitid fragments, the limestone is riddled with light grey, subcircular to ovoid "white spots" (some indicated by arrows) up to about 10 cm in size. Scale bar: 10 cm.

low water energy. Such environments are characteristic of inner banktop areas of isolated carbonate platforms (e.g. Wilson, 1975), but may also be established in sheltered areas close to platform margins (e.g. Colby and Boardman, 1989).

5. Facies associations

5.1. Description

At Cava Romana, the succession of the main quarry is dominated by rudist-clastic grainstones to packstones, with intercalated rudist biostromes a few decimetres to about 1.5 m thick (Fig. 4A). The lowermost interval 1 appears parallel-bedded, and consists mainly of bioclastic limestones. At its top, a biostrome about 30 cm thick of *Radiolites* bafflestone is present (Fig. 5). This biostrome is capped by a sharply defined surface with a slightly irregular small-scale relief (see below for further description). This surface, in turn, is overlain by bioturbated, fine-grained bioclastic packstone with floating, large rudist fragments at the base of the succeeding interval 2.

Interval 2 consists of subparallel-bedded, rudist-clastic packstone to grainstone interlayered with rudist biostromes with an open, parautochthonous fabric. Subordinately, bioclastic wackestone is

present. The biostromes are mottled by the darker fills of the firmground burrows. Each biostrome seems to be covered by a relatively thin interval of bioclastic limestone which, in turn, is topped by a faintly visible, but apparently sharply defined surface with an irregular small-scale relief (see below for further description). Over the distance of exposure in the quarry wall, an estimated hundred metres, the surfaces are subparallel to bedding. In the blocks stored aside the quarry, sharply defined surfaces in close vertical association to rudist biostromes with an open, parautochthonous fabric are present (Figs. 7, 10–12).

Interval 3 is dominated by subparallel-bedded bioclastic limestones. In the upper part, three rudist biostromes with an open, parautochthonous fabric are present; the lowest biostrome pinches out within the quarry (Fig. 4A). Each biostrome is riddled with the described firmground burrows. Aside the quarry pit, blocks are stored that contain an interval of rudist floatstone with a well-developed burrow network filled with grey packstone to grainstone. This floatstone interval is topped by a surface with a sharply defined, irregular topography (Fig. 11). This suggests that at least one of the biostromes in interval 3 is topped by a sharp, irregular surface. The topmost interval 4 (Fig. 4A) consists of rudist-clastic grainstones. In its lower part, it is built by stacked sets of oblique-tangential cross-beds up to several decimetres in height, and by sets of bidirectional cross-laminae. The upper part is a set a few metres thick of gently unidirectionally inclined beds of bioclastic grainstone.

In Cava Cortese (Fig. 4B), the lowermost interval 1 of bioturbated bioclastic wackestone to packstone grades up-section into interval 2, a package of bioclastic wackestone to packstone with intercalated layers of radiolitid-clastic floatstone. Higher up, the intervals of wackestone to packstone disappear and the overall content of radiolitid fragments increases. The topmost interval 3 consists of floatstone to rudstone composed mainly of platy, calcitic radiolitid fragments and "white spots" that are interpreted as ghost structures of radiolitids (Fig. 9B; see below for further description).

5.2. Interpretation

At Cava Romana, the dominance of bioturbated to cross-laminated and cross-stratified, shallow-water bioclastic grainstones to packstones indicates deposition in an open, shallow subtidal environment with medium to intermittently high water energy. The bedset of cross-laminated rudist-clastic grainstone (interval 4) was deposited from a carbonate sand body that shoaled into fair weather wave-base. The rudist biostromes, by contrast, probably accumulated under moderate to low water energy. At Cava Cortese, the upward coarsening from rudist-clastic wackestone (interval 1) into floatstone and rudstone (interval 3) may record progradation of a bank of lime mud colonized by radiolitids. Because of the common radiolitid ghost structures (see below) in interval 3, the floatstone to rudstone was deposited from a radiolitid level-bottom, or a biostrome with an open, parautochthonous fabric. Radiolitid biostromes typically accumulated in areas of moderate to low water energy, in lagoons or in sheltered areas close to platform margins (e.g. Sanders, 1996; Moro, 1997).

6. Emersion surfaces

6.1. Description

The blocks stored aside the quarry indicate that the mentioned, sharply defined surfaces are present either closely below a rudist biostrome (Fig. 7) or, most commonly, above a biostrome, or cap it (Figs. 5, 10–12), or are intercalated between successions of bioclastic grainstones to packstones. The limestones that overlie the surfaces most commonly are rudist-clastic grainstones to packstones with floating rudists or, rarely, bioclastic wackestones to floatstones.

The surfaces are sharply defined both in field and thin section, and show a rugged small-scale relief with a local amplitude of a few millimetres to a few centimetres to, locally, more than a decimetre (Fig. 11). Along the surfaces, the topmost millimetre of the underlying limestone typically is micritized (Fig. 12A). The underlying limestone locally shows steep-sided to overhanging walls up to a few centimetres in height. Below some of the surfaces, original lime mud was replaced by microsparite to pseudosparite (Fig. 12B). Downward, the sparitization gradually disappears within less than a centimetre to a few centimetres. The surfaces truncate both rudist shells and the firmground burrow fills

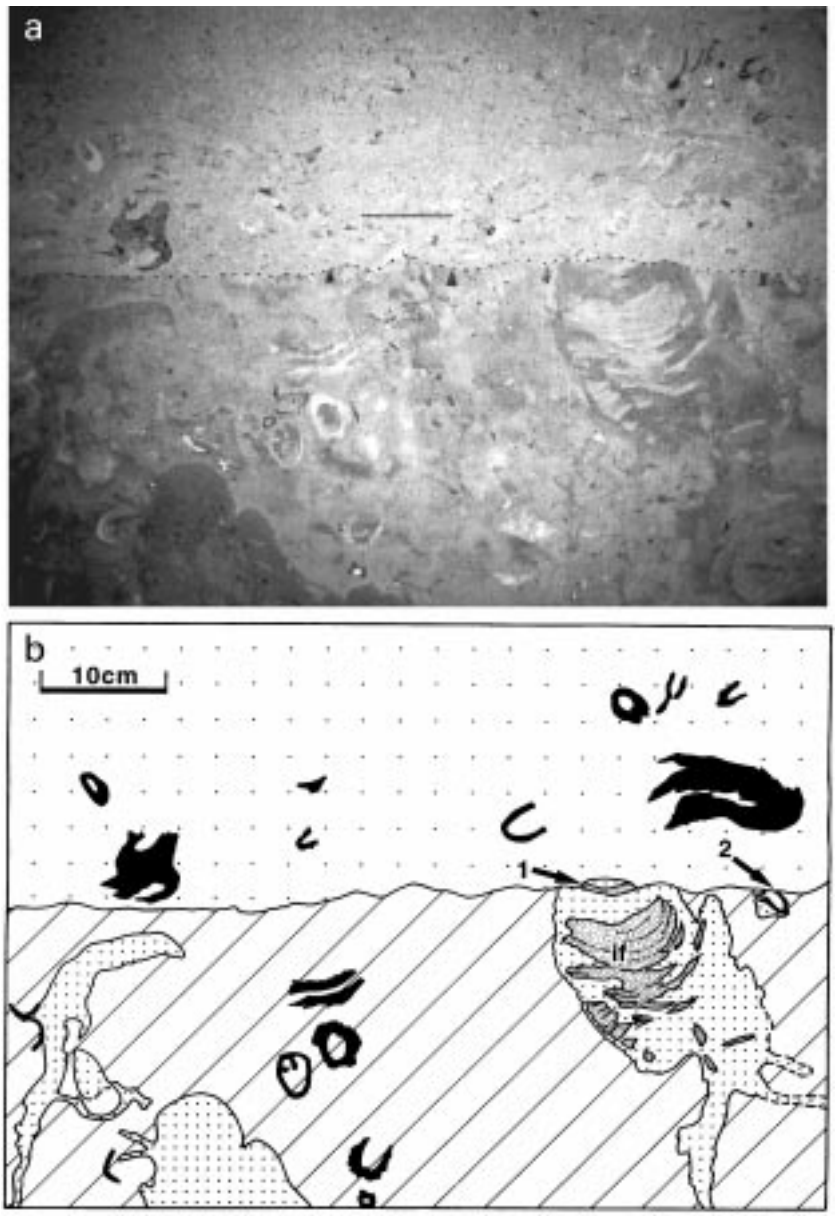

Fig. 10. Photograph and line-drawing of a biostrome with an open, parautochthonous fabric, cut perpendicular to bedding. Rudist shells and large shell fragments shown black. The lower part of the photo shows a bioturbated bioclastic wackestone to packstone (cross-hatched) with a few floating, disoriented shells of hippuritids and radiolitids. In addition, patches of darker-coloured bioclastic packstone (stippled) are present. Right of centre, the large patch contains abundant floating, crescent-shaped, light grey components of fine-grained bioclastic wackestone to packstone (if; fine stipples). The interval is capped by a hardground (fine stipples) that truncates all lithologies (arrow 1) and fossils (arrow 2). The hardground is overlain by very poorly sorted rudist-clastic packstone to grainstone with floating, large shell fragments.

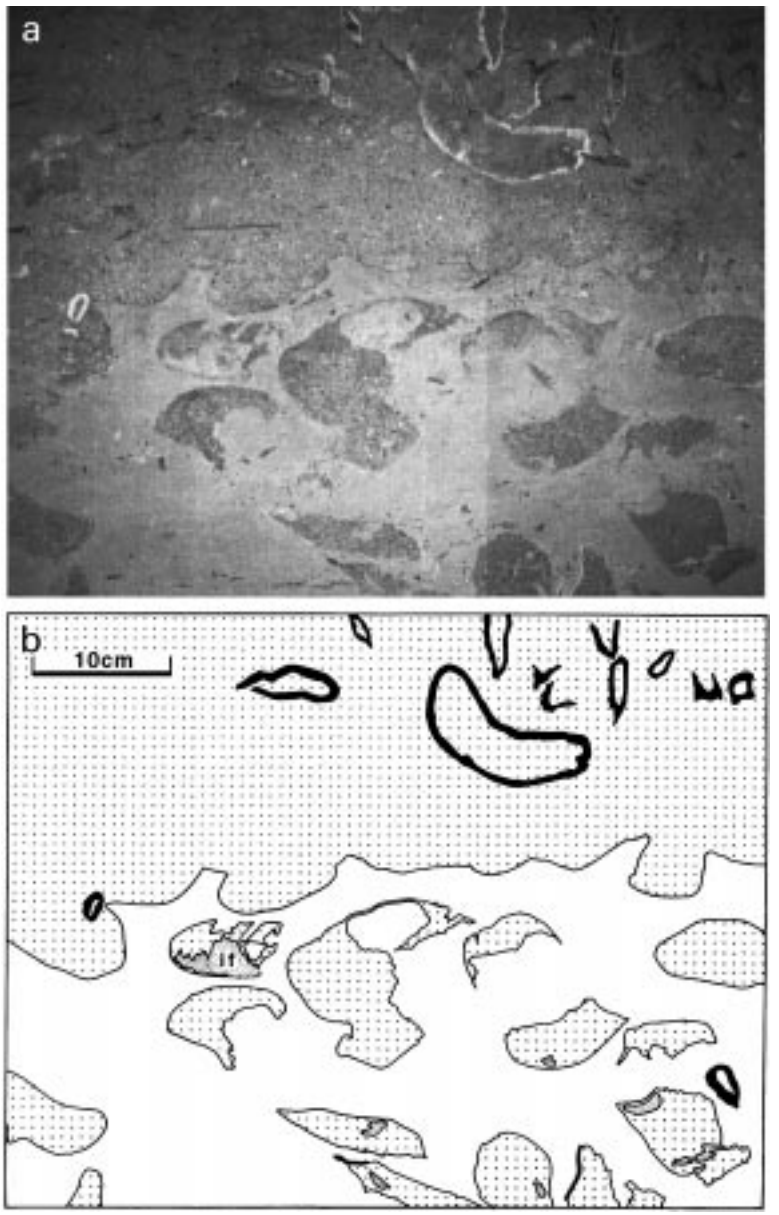

Fig. 11. Photograph and line-drawing of a surface cut perpendicular to bedding. Rudist shells and large shell fragments shown black. The lower part of the block consists of light grey, bioturbated packstone to wackestone (white) that is riddled with sharply bound cavities filled with darker grey, coarse sand rudist-clastic grainstone (stippled). In the grainstone, angular clasts and "serrated" patches of light grey lime mudstone to fine-sand bioclastic wackestone (fine stipples) are present of locally crescentic shape, or are arranged into stacks of crescents (if). The biostrome is topped by a hardground with deeply rugged morphology. The hardground is overlain by a coarse-sand rudist-clastic packstone to grainstone (stippled) with rudists that are embedded either upright or disoriented. The packstone to grainstone above the hardground is of the same colour, mean grain size and composition as the grainstone that fills the cavities in the underlying limestone.

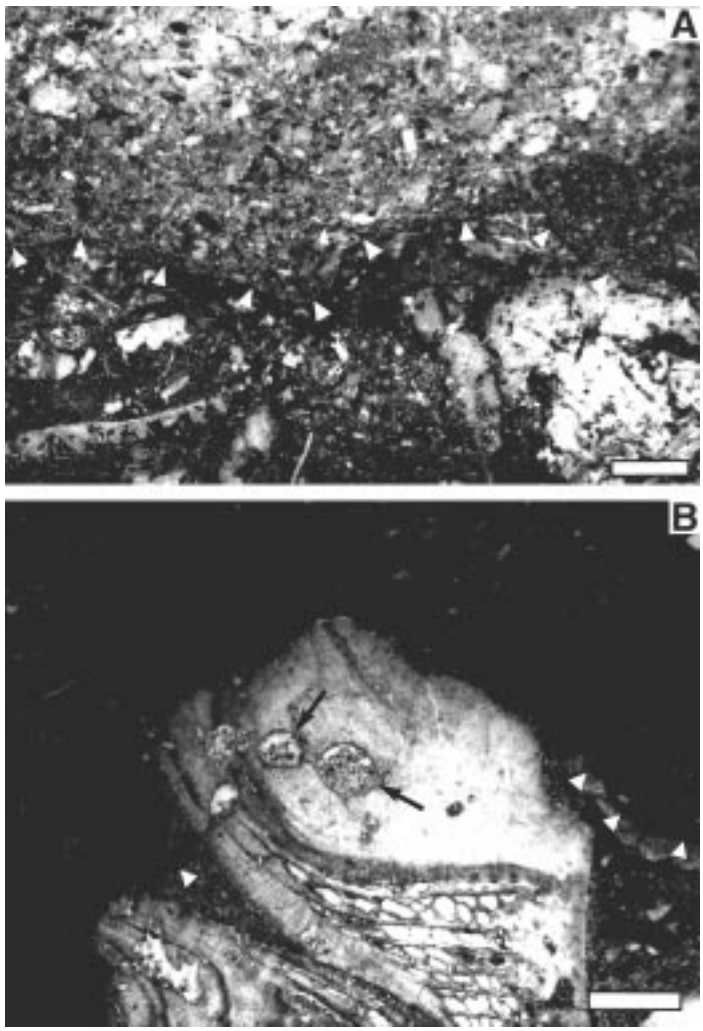

Fig. 12. (A) Hardground (indicated by white arrowtips) on top of very poorly sorted bioclastic wackestone. The hardground bears a thin micrite crust. The overlying limestone is a moderately sorted biclastic packstone. Scale bar: 2 mm. (B): Large radiolitid shell fragment, truncated along a hardground (portions where hardground tops the matrix of the underlying limestone indicated by white arrowtips). Note the borings in the radiolitid shell that are geopetally filled with grainstone (arrows) composed of fine sand- to silt-sized components. The overlying limestone is a fine sand bioclastic packstone rich in smaller benthic foraminifera (hardly visible in photograph because of contrast in light transmittance). Scale bar: 2 mm.

(Figs. 10–12). Where an interval of bioclastic grainstone is topped by such a surface, the grainstone closely below contains pendant micritic cement and/or meniscus cement, locally overlain by lime mudstone to microbioclastic packstone within the remnant pore space; moreover, a portion of the sand-sized components may have been replaced by lime mudstone to microbioclastic packstone. Where packstones are topped by such a surface, the diagenesis immediately below does not differ from the diagenesis of packstones farther below.

6.2. Interpretation

The described surfaces represent emersion surfaces, as indicated by their sharp outline, their rugged small-scale relief, truncation of both fossils and burrow fills, by pendant cement and/or meniscus

cement closely below a surface, and by dissolution mainly of aragonite, in contrast to the rudist shells above a surface. Below the surfaces, the sand grains replaced by lime mudstone to microbioclastic packstone probably represent biomoulds of aragonitic grains that were dissolved during subaerial exposure. Stable isotope data also support an interpretation as emersion surfaces (see below). In the storage aside the quarry, blocks of bioclastic grainstones with intercalated emersion surfaces are present, but even when wet the surfaces show quite faint because of the uniform colour of the limestone throughout. It is, thus, possible that the grainstones to packstones within the intervals 1 to 3 (Fig. 4A) contain emersion surfaces that went unidentified by inspection from distance. Therefore, the succession was not described and interpreted in terms of upward shoaling cycles. The emersion surfaces may have formed as a result of small changes in relative sea-level. On top of partly emergent sand shoals and skeletal mounds, freshwater lenses less than a metre to a few metres in depth and of limited lateral extent form. Freshwater input is sufficient for aragonite dissolution and aragonite–calcite transformation in a shallow, meteoric-vadose to mixing-zone phreatic diagenetic environment, and for the formation of an emersion surface (e.g. Harris, 1979; Budd, 1988).

7. Diagenesis

7.1. Petrography

A summary of the diagenetic evolution of the limestones from Cava Romana is shown in Fig. 13. In interstitial pores and/or in intraskeletal pores of rudists, the lowermost cement locally is a thin, isopachous fringe of radial-fibrous acicular calcite, or palisad cement. In a few samples, first cementation is recorded by micritic pendant cement, micritic cement fringes, and meniscus cement. Aragonitic bioclasts became replaced either by blocky calcite

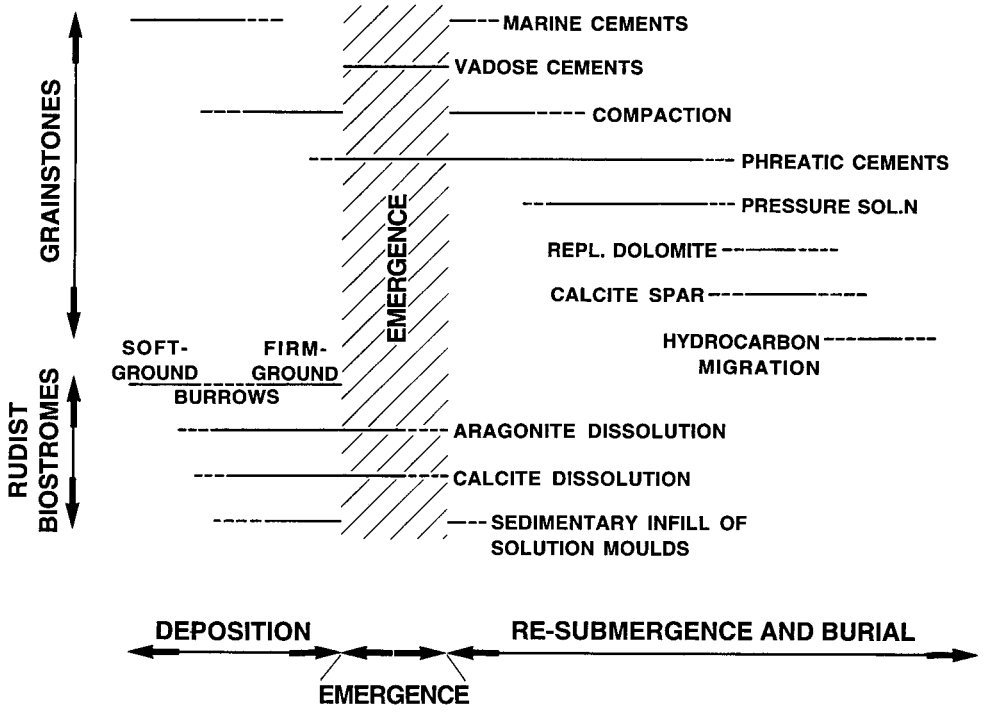

Fig. 13. Summary of diagenesis at Cava Romana. Above: Diagenesis recorded in bioclastic grainstones. The relative time of precipitation of replacement dolomite and of coarse calcite spar in open pores (fractures, biomoulds) is poorly constrained. Below: Processes and early diagenetic phenomena important for taphonomy of rudist biostromes. See text for further description and discussion.

spar, or by lime mudstone to microbioclastic wacke/packstone. Commonly, grainstones are cemented by an isopachous fringe of dog-tooth spar and/or, most commonly, by blocky calcite spar. Several samples of bioclastic grainstone lithified mainly by grain–grain pressure solution. Overall, the grainstones are densely packed, and cement is volumetrically subordinate. In the rudist biostromes, a minor amount of compaction-induced deformation of burrow-fills was locally observed. In some samples of bioclastic packstone and wackestone a few percent of small, disseminated, subhedral to euhedral dolomite crystals are present. Locally, the limestones are cut by fractures up to a centimetre in width. The fractures as well as, locally, the inner void of rudist shells are filled with milky to limpid, coarse calcite spar. In addition, large open pores built by rudist shells are present; these pores are partly filled with an internal breccia derived from the former sedimentary infill of the rudist shell and, locally, by corroded coarse calcite spar. In most of these open pores, stains of pyrobitumen are present (Fig. 14).

At Cava Cortese, diagenesis as deduced from thin-sections records early dissolution of radiolitids (described further below), and compaction and lithification of the lime mud matrix. Because of the pure carbonate composition, no stylolites or solution seams developed. In bioclastic packstones and wackestones from interval 1 small, disseminated, subhedral to euhedral dolomite crystals locally comprise up to about 15% of the rock.

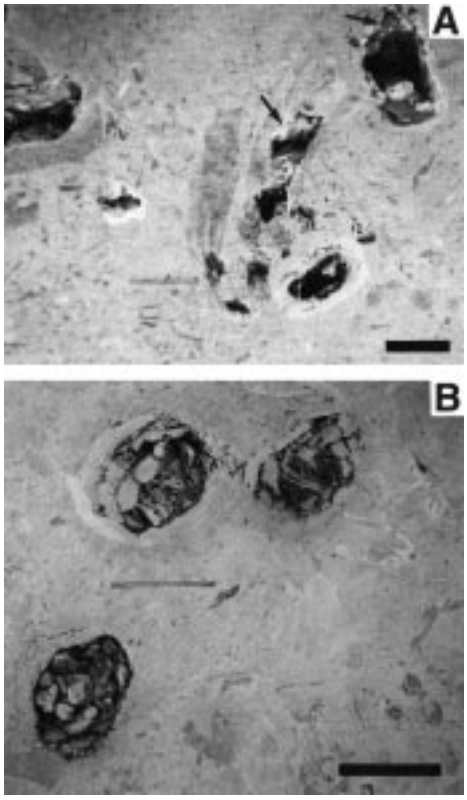

Fig. 14. Macropores in rudist biostromes. (A) Pores several centimetres wide produced by the inner cavity of rudist shells. Within the pores, locally corroded remnants of coarse calcite spar (arrows) are present, and are overlain by a stain of pyrobitumen. Scale bar: 2 cm. (B) Pores in the inner cavity of poorly preserved rudists. The pores are partly filled with an internal breccia composed mainly of the lithified intertabular fills of the lower rudist valve. Scale bar: 5 cm.

7.1.1. Interpretation

The isopachous fringes of radial-fibrous, acicular cement or of palisad cement that locally build the first cement precipitated in a marine-phreatic environment. The micritic pendant cements and meniscus cements, by contrast, formed in the meteoric-vadose zone. The biomoulds filled with lime mudstone to microbioclastic packstone record aragonite dissolution in a meteoric-vadose/phreatic environment, followed by infill with marine-derived sediment. Both the fringes of dog-tooth spar and the blocky calcite spar formed in a phreatic environment. Mechanical compaction overlapped, in its late stage, with the sedimentary infilling of the burrow networks. The fractures filled by the coarse calcite spar formed when the limestone was sufficiently lithified for brittle deformation. No cross-cutting between the disseminated replacement dolomite and the calcite spar was found to deduce their relative time of formation. The pyrobitumen in the pores built by rudist shells may represent a vestige of hydrocarbons. Early diagenesis of the bioclastic wacke/packstones to floatstones was characterized by compaction, by mineralogical stabilization of lime mud and, probably, by cementation (cf. Shinn and Robbin, 1983; Lasemi et al., 1990; Goldhammer, 1997). Some volume loss of the pure lime mud may have been produced by "pervasive" pressure solution (Wanless, 1979). The good preservation of rudist relicts (see below) in floatstones, however, suggests

that pressure solution led not to significant volume loss along discrete surfaces.

7.2. Stable isotopes

Stable isotopes of oxygen and carbon of selected samples were measured to check diagenetic overprint and the interpretation of the emersion surfaces (Table 1). Most isotope ratios plot between +2 to +3‰ δ^{13}C and −2 to −3.5‰ δ^{18}O PDB (Fig. 15). This fits ratios from limestones that underwent meteoric to mixed marine-meteoric diagenesis (e.g. Hudson, 1975; Allan and Matthews, 1977, 1982; Minero, 1991; Immenhauser et al., 1999). During diagenesis, the low-Mg calcitic (ostracal) parts of rudist shells probably suffered only limited isotopic exchange (Woo et al., 1993; Steuber, 1999). Because the bulk limestone samples consist mainly of calcitic rudist fragments and are typically poor in cement, the crowding of the isotope ratios of rudist shells and bulk sediment seems a consequence.

From three emersion surfaces checked, two show a shift from relatively "light" isotope ratios in the sediment immediately below the surface (B in Fig. 15) to "heavier" ratios above (A in Fig. 15). Across exposure surfaces, the range of δ^{13}C and δ^{18}O may be wide both within a section and among different sections. It is mainly the shift of isotope ratios across a surface and not, within reasonable limits, their absolute values that indicate meteoric diagenesis (Allan and Matthews, 1982, Fig. 4 ff.; Immenhauser et al., 1999). The difference between the isotope ratios of the bulk sediment closely below the emersion surfaces and of limestones some distance away (unlabelled black dots in Fig. 15) suggests that the shift to lower values is confined to the interval closely below the exposure surface (see also Allan and Matthews, 1982; Immenhauser et al., 1999).

The third surface, although conspicuous in field and thin-section (Fig. 12B), showed no isotope shift across (bulk sediment samples indicated by small arrows in Fig. 15). The sediment below this surface may have received little meteoric overprint because of a low topographic position, i.e. only a very thin vadose or mixed vadose-marine zone had developed. Alternatively, the isotope ratios closely below the surface may have been overprinted by isotopically "heavy" marine waters during subsequent transgression.

Two of the three samples from coarse calcite spar plot into the field of rudist shells that probably reflects a high retention of the original isotope ratio. The third sample plots at slightly negative δ^{13}C. These isotope ratios may suggest that the coarse calcite spar was precipitated from marine to mixed marine-meteoric waters (cf. Immenhauser et al., 1999). Although more samples of coarse calcite spar are needed to test this hypothesis, it seems to be supported by very low Fe and Mn versus high Sr values in the calcite (see below).

7.3. Trace elements

None of the cements showed cathodoluminescence, except for very dull luminescence of a few echinoderm grains and bright orange luminescence of very rare, calcite-filled microcracks. All the samples have low contents of Fe and Mn versus significantly higher Sr (Table 2). Although Fe is less than 1400 ppm, the Mn is either below or within the range of 20–225 ppm where luminescence or non-luminescence may occur in natural calcites (Savard et al., 1995). The reasons for non-luminescence, as judged by the human eye (Haberman et al., 1998), at such concentrations are poorly known (Savard et al., 1995).

With increasing water/rock ratio, at limited supply of Fe and Mn, and under oxidizing conditions, a diagenetic system tends to open successively with respect to ^{18}O, ^{13}C, Sr, Fe and Mn (Banner and Hanson, 1990; Woo et al., 1993). Moreover, the uptake of trace elements into calcite is controlled by several variables (T, composition of the solution, reaction kinetics, pressure), and the distribution coefficients are poorly constrained (e.g. Brand and Veizer, 1980). These factors all detract from the quantitative interpretability of trace element contents.

The Friuli platform was an isolated carbonate shelf, and the investigated part of the Borgo Grotta Gigante Member is underlain by about 3000 m of shallow-water carbonates (cf. Cati et al., 1987). Thus, no source of terrigenous iron and manganese was present. The consistently low contents of Fe and Mn, also in the coarse sparry calcite, and the

Table 1
Stable isotope ratios of carbon and oxygen. Where two measurements were made, in Fig. 15 the average of the two measurements is plotted. Key: infill = limestone infill of rudist ghosts; H. = *Hippurites*

Sample	Nature	$\delta^{13}C$	$\delta^{18}O$	Remarks
1700 S	Bulk sediment	4.284 PDB	−2.861 PDB	
		4.303 PDB	−2.725 PDB	
1707 A/S	Bulk sediment	2.529 PDB	−2.901 PDB	
		2.543	−2.788 PDB	
1715 S	Bulk sediment	2.705 PDB	−2.226 PDB	With 14.4% dolomite
1716 S	Bulk sediment	2.510 PDB	−2.846 PDB	
		2.536 PDB	−2.739 PDB	
1724 S	Bulk sediment	2.579 PDB	−2.776 PDB	
		2.599 PDB	−2.590 PDB	
1712 M	Bulk wkst. matrix of biostrome	4.170 PDB	−3.024 PDB	
		4.212 PDB	−2.948 PDB	
1720 S/BE	Bulk sediment below hardground	2.268 PDB	−5.816 PDB	
		2.195 PDB	−5.865 PDB	
1720 S/AB	Bulk sediment above hardground	2.516 PDB	−2.522 PDB	
		2.556 PDB	−2.450 PDB	
1729 S/BE	Bulk sediment below hardground	0.603 PDB	−7.303 PDB	
1729 S/AB	Bulk sediment	3.151 PDB	−3.463 PDB	
	above hardground			
		3.153 PDB	−3.427 PDB	
1730 S/BE	Bulk sediment below hardground	2.613 PDB	−2.744 PDB	
1730 S/BE2	Bulk sediment below hardground, 2nd sample	2.561 PDB	−2.770 PDB	
1730 R/BE	Radiolitid ostracum below hardground	2.103 PDB	−2.569 PDB	
1730 S/ AB	Bulk sediment above hardground	2.444 PDB	−2.740 PDB	
1716 B	Biocl. limestone infill	2.610 PDB	−2.840 PDB	
		2.641 PDB	−2.789 PDB	
1724 M	Mudstone infill	3.687 PDB	0.369 PDB	
1727 B/M	Mudstone infill	2.491 PDB	−3.212 PDB	With 0.6% dolomite
		2.438 PDB	−3.243 PDB	
1707A/R	Radiolitid ostracum	2.264 PDB	−3.191 PDB	
		2.294 PDB	−3.126 PDB	
1718 R	Radiolitid ostracum	2.536 PDB	−2.734 PDB	
		2.630 PDB	−2.453 PDB	
1719 R	Radiolitid ostracum	2.155 PDB	−2.884 PDB	
		2.045 PDB	−3.103 PDB	
1720 R	*H. nabresinensis*	2.025 PDB	−2.951 PDB	
		2.034 PDB	−2.717 PDB	
1724 R	Radiolitid ostracum	2.069 PDB	−3.144 PDB	
		2.063 PDB	−3.087 PDB	

Table 1 (*continued*)

Sample	Nature	$\delta^{13}C$	$\delta^{18}O$	Remarks
1727 B/R	Radiolitid ostracum	2.609 PDB	−2.382 PDB	
		2.582 PDB	−2.668 PDB	
1729 R	*H. nabresinensis*	2.143 PDB	−2.803 PDB	
1707 A/C	Coarse calcite	−0.019 PDB	−3.138 PDB	
		−0.002 PDB	−3.143 PDB	
1720 C	Coarse calcite	2.882 PDB	−2.661 PDB	
1729 C	Coarse calcite	2.842 PDB	−2.560 PDB	

substantially higher Sr suggest that the diagenetic system was open (or rock buffered) for Sr but closed for, or starved of, Fe and Mn (e.g. Woo et al., 1993; see also Budd, 1997, p. 32). In oxygenated marine waters, dissolved Fe^{2+} averages 2×10^{-3} ppm, ranging between 1×10^{-4} and 6×10^{-2} ppm (Holland, 1978). The distribution coefficient of iron into calcite is estimated at 1 to 20 (Brand and Veizer, 1980, Fig. 1). In oxygenated marine waters, most Mn is present as manganese oxides, at an average of dissolved Mn^{2+} of 2×10^{-4} ppm, and a range from 5×10^{-5} to 8.8×10^{-4} ppm (Holland, 1978, Table 5.2). Suggested values for the distribution coefficient of Mn into calcite range from 5.4 to 1700 (Brand and Veizer, 1980, Fig. 1). Under reducing conditions, iron precipitates mainly within pyrite while the manganese oxides are reduced, thus increasing the content of dissolved Mn^{2+} available for incorporation into calcite (Lynn and Bonatti, 1965; Czerniakowski et al., 1984). Calcite precipitated from reducing marine

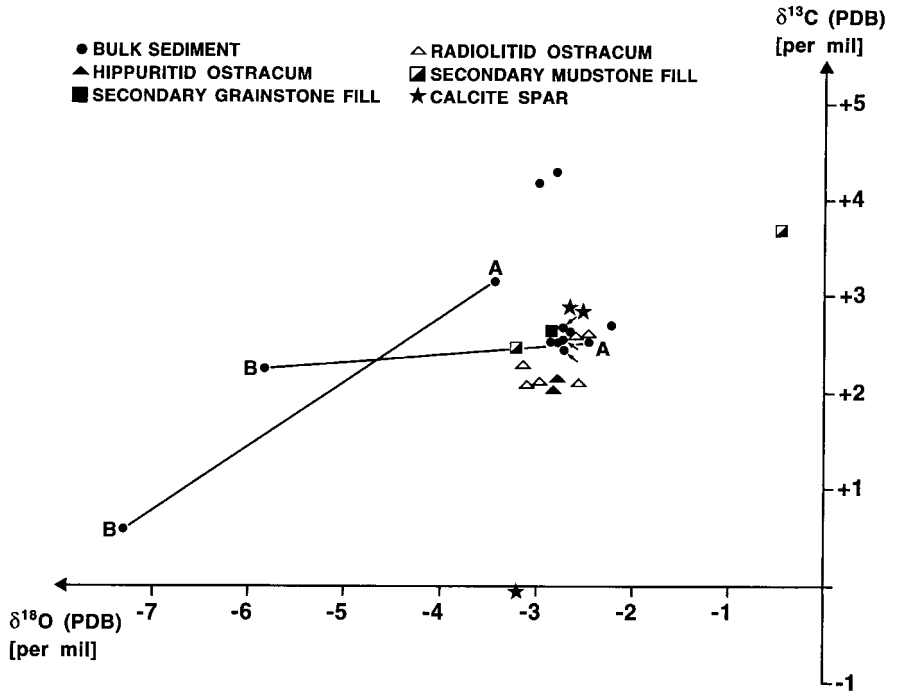

Fig. 15. Stable isotope ratios of oxygen and carbon. Connected pairs B–A indicate isotope ratios of bulk sediment immediately below a hardground (B) and bulk sediment closely above the same hardground (A). In one case, the isotope ratios of the bulk sediment immediately below and above a hardground plot within a narrow range (dots indicated by small arrows). See text for further description and discussion.

Table 2
Contents of Fe, Mn and Sr of selected samples. Key to indices: BE = Below hardground (emersion surface); AB = Above hardground (emersion surface); Avg. = Average of several measurements; H. = *Hippurites*

Sample	Nature	Fe (ppm)	Mn (ppm)	Sr (ppm)	Remarks
1700	Bulk sediment	24	6	826	
1707a	Bulk sediment	33	6	469	
1709	Bulk sediment	173	58	174	
1712	Bulk sediment	88	33	1660	
1716	Bulk sediment	200	42	1284	
1720S/BE	Bulk sediment	43	8	526	
1720S/AB	Bulk sediment	58	13	917	
1724	Bulk sediment	18	6	294	Avg. of 2
1729S/BE	Bulk sediment	34	4	181	Avg. of 2
1729S/AB	Bulk sediment	52	7	398	
1730S/BE	Bulk sediment	12	2	141	Avg. of 3
1730S/AB	Bulk sediment	28	1	131	
1706	Mudstone fill	160	59	1949	
1724	Mudstone fill.Fill	381	77	1659	
1727b	Mudstone fill	184	80	2268	
1716	Bioclast. limest. Fill	274	61	2225	
1707a	Radiolitid ostracum	7	5	546	
1718	Radiolitid ostracum	3	4	211	
1719	Radiolitid ostracum	115	55	2742	
1720	*H. nabresinensis*	10	6	300	
1727b	Radiolitid ostracum	28	25	1498	
1728	*H. nabresinensis*	47	8	375	
1729	*H. nabresinensis*	2	3	217	
1730	Radiolitid ostracum	3	<1	970	
1707a	Coarse calcite	3	29	1052	
1720	Coarse calcite	6	69	2124	Avg. of 3
1729	Coarse calcite	50	11	408	

pore waters thus is most commonly luminescent (e.g. Czerniakowski et al., 1984). The small amount of Mn both in the bulk sediment and in the coarse calcite spar indicates that the pore waters were either very poor in Mn (meteoric waters), and/or were oxygenated.

The ostracal parts of rudist shells and the four measured limestone fills of rudist biomoulds are characterized by low and similar contents of Fe and Mn, and high values of Sr. Low Mg-calcite shells are characterized by a relatively high retention of their original trace element content (Al-Aasm and Veizer, 1986; Woo et al., 1993; Steuber, 1999). Both rudist shells and limestone infills thus may represent more-or-less closed small-scale diagenetic systems with high retention. The contrasting trace element contents of rudist shells and infills versus the bulk sediment thus is consistent with earlier meteoric overprint of the bulk sediment (cf. Al-Aasm and Veizer, 1986; Woo et al., 1993). For the coarse calcite spar, the low Fe + Mn/high Sr and, for one sample, the slightly negative $\delta^{13}C$ suggest precipitation in oxygenated marine to mixed marine-meteoric waters (e.g. Woo et al., 1993).

8. Taphonomy of rudist biostromes

8.1. Construction of the radiolitid shell

Radiolitid shells consist of a calcitic ostracum and an aragonitic hypostracum (Kennedy and Taylor, 1968; Skelton, 1974). The attached valve of many radiolitids is built by: (1) an outermost ostracal layer that commonly is less than 1 mm thick and that

consists of stacked, delicate calcite lamellae; (2) an ostracal shell layer ("boxwork ostracum") up to more than 10 cm thick that consists of numerous hollow "boxes" up to 1 mm in width that are built by horizontal, radial funnel plates and vertical cell walls; (3) an "inner ostracal layer" about 0.5 to 4 mm thick of thick-walled boxwork or of massive calcite; and (4) the hypostracum that formed the innermost shell layer and the tabulae. In the free valve, the ostracum consists of two layers (a) an inner layer of calcite that appears poorly structured under the optical microscope, and (b) an outer layer composed of stacked calcite lamellae; the hypostracum built the inner shell layer, including the teeth and the myophores (see Skelton, 1974; Amico, 1978; Pons and Vicens, 1986; Sanders, 1999, for further descriptions of the radiolitid shell).

8.2. Cava Romana

In the biostromes of the main quarry, preservation of radiolitids in upright position, with all the shell layers (hypostracum always preserved as blocky calcite spar), and with the upper valve is relatively rare. On many radiolitids, chunks of boxwork ostracum were spalled off the inner ostracal layer, leaving a sharp gap. Locally, in the biostrome matrix, large pieces of boxwork ostracum are embedded near attached radiolitid valves that are partly dismantled from their boxwork layer (see Sanders, 1998, plate 5; Sanders, 1999, figs. 4 and 5B, for examples from Cava Romana). Alternatively, the boxwork layer was uniformly thinned over the entire shell perimeter. On many radiolitids, removal of the boxwork layer was complete. The radiolitids partly or completely dismantled from their boxwork ostracum are preserved either reoriented, or are embedded in upright position.

Within the biostromes sharply defined tubes are present that are bounded towards the host limestone by a layer 1–3 mm thick of calcite. In longitudinal section, the tubes are a few centimetres to 10–30 cm in height, and typically are of elongated cone shape. In transverse section, the "calcite tubes" show a subcircular to heart-like shape (Fig. 16A), and many of the tubes show a characteristic doubling of the calcite layer. The doubled calcite layer forms a lamella that may extend for up to about 1 cm into the lumen of the tube, and is split at its end. In thin-section, the calcite layer that forms the tubes shows an internal structure identical to the inner ostracal layer of radiolitids, i.e. either a thin layer of massive calcite or a single layer of thick-walled boxwork. In many cases, the calcite layer is directly connected with preserved portions of the boxwork ostracum (Fig. 17A). The calcite tubes are either filled with the matrix limestone of the biostrome, or by the same dark grey bioclastic packstone to grainstone that fills adjacent burrows. Aside from the calcite tubes, attached radiolitid valves with more-or-less intact boxwork ostracum and inner ostracal shell layer are present, and that are filled with the dark grey bioclastic limestone of the burrows; within these radiolitid shells, no vestige of the formerly aragonitic, hypostracal shell was recognized.

Another feature of the biostromes are crescent-shaped sediment bodies typically a few centimetres in length and a few millimetres to 1.5 cm thick. These "crescents" consist of lime mudstone to wackestone to fine sand bioclastic packstone. Locally, within single crescents, a geopetal interlamination of lime mudstone, wackestone and packstone is observed. The crescents commonly are stacked into arrays up to about 20 cm in length (Figs. 16B–D and 18). Between the crescents of a stack, layers about 1 mm thick of lime mudstone to fine sand bioclastic wackestone to packstone are present that sharply define the crescents' outlines (Fig. 16B). Stacked crescents are present either within calcite tubes as described, or are surrounded by a tubular rim a few millimetres to a few centimetres thick (Fig. 16B). The rim is filled with lime mudstone to bioclastic wacke/pack/grainstone. The limestone within the rim is in physical continuity with, and typically of identical composition as, the thin limestone layers that vertically separate the crescents of a stack (Fig. 18). Within the fill of a rim, a geopetally oriented textural variation of the limestone may be present.

Locally, stacked crescents appear to float within the grey packstone to grainstone of the burrow network (Figs. 8, 10 and 11). The floating stacks may be more-or-less disintegrated into single, disoriented crescents each of which, however, shows a sharp boundary towards the burrow fill. The crescent stacks are commonly oriented with their long axis subvertical to bedding (Fig. 16B–D and 18), but stacks oblique to subhorizontal to bedding also were observed. In compacted limestones, where the crescents are

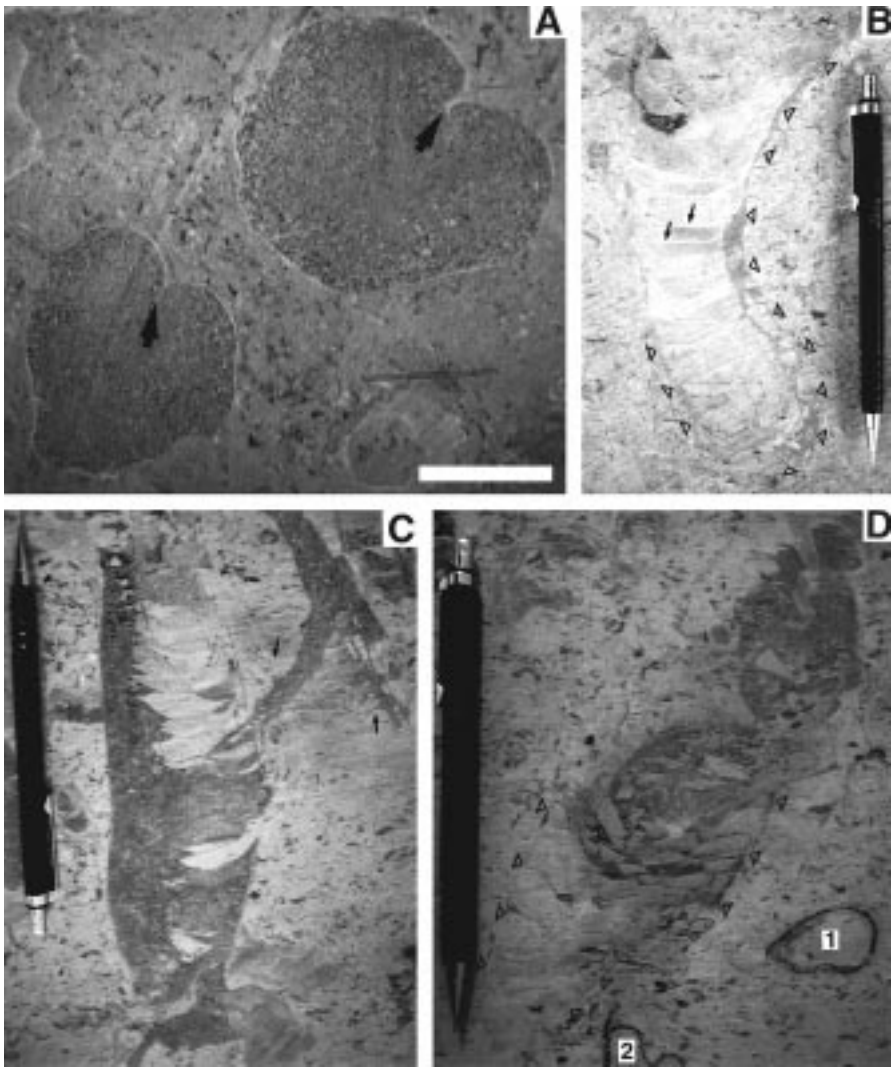

Fig. 16. Relict rudist preservation. (A) Two subcircular patches of dark grey, coarse sand bioclastic grainstone. The patches are bounded by a layer 2–3 mm thick of calcite. At one side, the calcite layer merges into a lamella that protrudes into the inner part (arrow) and, in turn, is split at its termination. Scale bar: 5 cm. (B) Array of stacked, crescent-shaped bodies that each consists of fine-grained bioclastic wackestone to packstone. The "crescents" locally are vertically separated by layers (indicated by small arrows) about 1–2 mm thick of light grey micro-bioclastic packstone. The stack of crescents is rimmed, over most of its extent, by a layer of darker grey bioclastic packstone (delimited by triangles). Pencil is 14 cm long. (C) Stack of light grey, crescent-shaped bodies of lime mudstone to bioclastic wackestone. The stack partly floats within dark grey bioclastic grainstone; the same grainstone fills a fracture that crosses the stack of crescents, from upper left to lower centre. The dark grey grainstone is bounded towards the matrix wackestone by a layer about 1.5 mm thick of shell calcite. Pencil is 14 cm long. (D) Stack, delimited by triangles, of indistinctly crescent-shaped bodies composed of lime mudstone to bioclastic wackestone. Note that the crescents are deformed and, in the centre of the photo, are disintegrated into sharply bound fragments. In the central and upper part, the dark grey area is a poorly sorted bioclastic grainstone with fragments from crescents. In the central part of the photo, pore space between the fragments is filled with coarse calcite spar. 1, 2: Compaction-deformed shells of *Hippurites nabresinenis*. Pencil is 14 cm long.

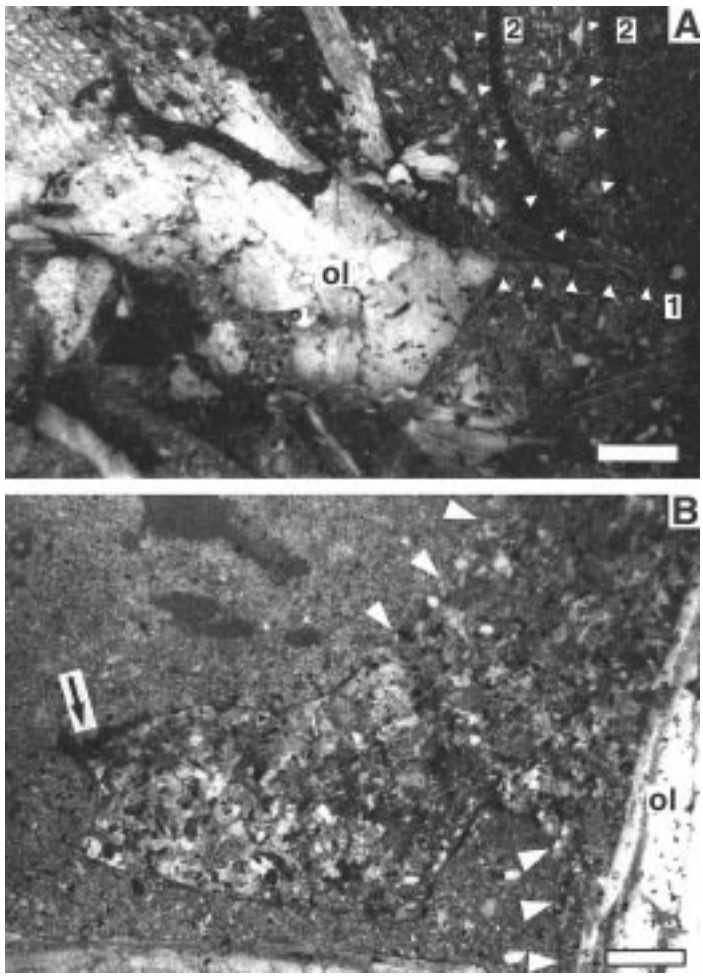

Fig. 17. (A) Oblique section through the calcitic, ostracal layer (ol) of lower radiolitid valve. The formerly aragonitic inner shell layer is not preserved, and the inner void of the radiolitid has been filled with silt-bioclastic packstone with a few rudist fragments. From the inner side of the thicker, calcitic part (ol) of the rudist shell, a thin calcitic shell layer (1, white arrowtips) extends farther towards the former shell commissure (to right). In the inner part of the radiolitid shell, two evenly thick layers of darker grey lime mudstone to microbioclastic packstones are present (2, white arrowtips) that curve towards the shell margin. Scale bar: 2 mm. (B) Longitudinal section through radiolitid with preserved upper valve (commissure to right). From the upper valve only the primary calcitic, ostracal shell layer (ol) is preserved. The inner, formerly aragonitic, hypostracal part (in part outlined by white arrowtips) was dissolved and became filled with bioclastic packstone. The shape of the dissolved shell part suggests that the section runs along a myophore of the upper valve. Note the thin micritic coat on the outer surface of the dissolved aragonitic shell part, and the irregularly shaped pendant (arrow) of lime mudstone of possible microbial origin. Scale bar: 2 mm.

preserved within calcite tubes or in rudist shells, they were crushed into angular fragments separated by open pores, by coarse calcite spar or by an intraclastic breccia cemented by calcite (Fig. 16D). Where the calcite tubes or the sediment rims that host the stacked crescents are filled with bioclastic grainstone, the grainstone rarely shows relicts of isopachous fringes of radial-fibrous cement. Most commonly, however, the grainstone is cemented by dog-tooth spar and blocky calcite spar, or by blocky calcite spar only.

8.2.1. Interpretation

The relatively rare in situ preservation of radiolitids with all shell layers and with the upper valve (Type A

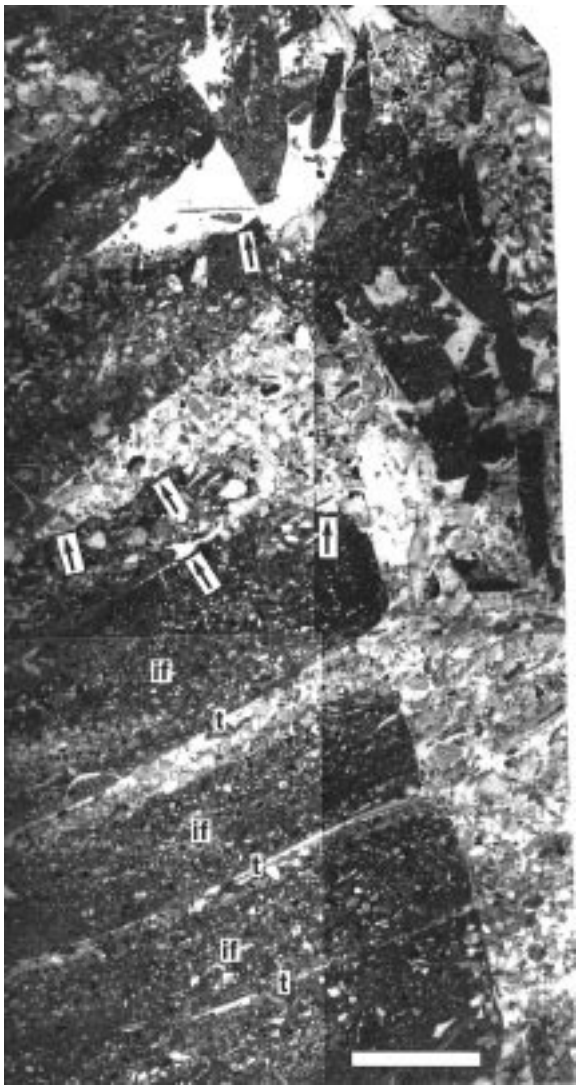

Fig. 18. Thin-section through relict of the attached valve of an elevator rudist. In its central part, the relict consists of the former intertabular fills (if) of microbioclastic wackestone. The intertabular fills are vertically separated from each other by layers of bioclastic packstone to grainstone that mark the formerly aragonitic tabulae (t). Upon dissolution of tabulae, the intertabular fills locally were welded to each other. The outer part of the rudist shell was dissolved, and became geopetally filled with rudist-clastic grainstone. The intertabular-fill limestone also was locally corroded, as indicated by the sharp, locally pitted and embayed boundary (arrows) between the intertabular fills and the grainstone. Dark grey, claviform patches of microbioclastic packstone in the upper right represent the fills of borings within the former rudist shell. Note that the fills are partly fragmented, and collapsed into the grainstone within the biomould. Scale bar: 5 mm.

preservation), the predominance of incompletely preserved radiolitids, and the burrow network all indicate that the biostromes were overprinted by taphonomic processes. Spalling of the boxwork layer off the inner ostracal layer, and the common presence of shell relicts composed of the inner ostracal layer suggest that disintegration was influenced by shell structure (cf. Sanders, 1999). Churning of both sediment and rudists by burrowing organisms and, possibly, repeated episodes of burial–exhumation of the rudists by bioturbation and physical sedimentary processes led to progressive abrasion and spalling of the ostracum.

The "calcite tubes" represent the inner ostracal shell layer of the lower valve of radiolitids. This is indicated by the attached relicts of boxwork ostracum, and by the identical structure of the calcite tubes with the inner ostracal layer of well-preserved radiolitids. In transversal section the double-layered, split-end calcite lamella represents the inner ostracal shell layer of the ligamentary crest, as evident in well-preserved specimens and in specimens that record intermediate stages of disintegration (cf. Sanders, 1999). Because they directly abut the limestone matrix, the relictic tube shells originated within the soft sediment. Relictic tube shells preserved disoriented (Type B preservation) may have been produced by both physical abrasion and spalling, in addition to dissolution. For the calcite tubes preserved in upright position and that directly abut the biostrome matrix (Type C preservation), the boxwork ostracum probably was removed by dissolution within the soft sediment. If the boxwork dissolved when the matrix was firm or lithified, there should be a gap between the relictic shell and the host limestone; such preservation is associated with another taphonomic history (see below). The sediment fill *within* type B and type C radiolitid relicts, respectively, is in contact with the inner ostracal shell layer. This indicates that the hypostracal aragonite had disappeared, most probably by dissolution, before sediment infill.

The stacked crescents of lime mudstone to wacke/pack/grainstone represent the fills of the intertabular chambers of the lower radiolitid valve. Identical "intertabular fills" are very common in well-preserved rudists (e.g. Cestari and Sartorio, 1995; Skelton et al., 1995; Sanders, 1999). The thin, even layers of lime mudstone to wackestone that separate the intertabular

fills from each other represent the former tabulae. The stacks of intertabular fills that are surrounded by a tube-shaped rim filled with lime mudstone to bioclastic grainstone represent the vestiges of radiolitids that underwent wholesale dissolution within the firm to lithified sediment (Type D preservation). The isopachous fringes of acicular cement in the sediment fill of radiolitid relicts probably precipitated in a marine-phreatic environment (e.g. Harris et al., 1985). Because the intertabular fills typically retained their shape even when floating isolated, and because they locally disintegrated into angular clasts, the fills were at least in a firm, semi-lithified state when the burrows became filled. Within the burrow fills, the upright stacks of intertabular fills strongly suggest that the rudist shell dissolved during and after burrow backfilling with sediment (Type E preservation). The stacks of intertabular fills aligned oblique to parallel to bedding were produced by toppling of the filled radiolitid shell, before aragonite dissolution.

8.3. Cava Cortese

The floatstone to rudstone of interval 3 (Fig. 4B) consists mainly of calcitic fragments of radiolitids and of "white spots" of lime mudstone to wackestone (Fig. 9B). The spots consist of stacked, crescent-shaped bodies each less than a centimetre to a few centimetres wide. In the stacks, the crescents are separated from each other by a layer less than a millimetre thick of lime mudstone to calcisiltite (Fig. 19A and B). These layers are in physical continuity with, and of identical colour to, the matrix wackestone to lime mudstone. In some stacks, the layers of lime mudstone between the crescents merge laterally into a layer of identical composition that runs along the flank of the stack (Fig. 19A). The stacked crescents commonly are more-or-less deformed by compaction, and/or are disintegrated into single crescents deformed by bioturbation and compaction (Fig. 19C). Some stacks oriented with their long axis oblique to parallel to bedding consist, either completely or in part, of "half crescents". The upper boundary of each half crescent is subparallel to bedding (Fig. 19C).

8.3.1. Interpretation

The stacked crescents of lime mudstone to wackestone represent the intertabular fills of radiolitids. The well-defined shape also of single intertabular fills and their moderate compactional deformation indicate that they were in a firm state when exposed in the sediment upon dissolution of their hosting radiolitid shells. In well-preserved stacks of intertabular fills, the laminae of lime mudstone to calcisiltite that separate the intertabular fills and that are laterally connected to each other along one or both sides of the stack represent the former tabulae and the aragonitic layer on the inner side of the attached valve. Shell dissolution was complete at least for the aragonitic parts of the lower valve. The near absence of relict ostracal shell layers as found in Cava Romana, and the paucity of larger clasts of boxwork ostracum suggest that the ostracal shell layer, too, may have been dissolved within the sediment, and/or the radiolitids were more-or-less dismantled of their boxwork before final embedding (Sanders, 1999). If the lower valves were all preserved, interval 3 of Cava Cortese would be classified as a biostrome with a parautochthonous, open fabric. This interval thus provides an example for a "ghost biostrome". Only the relatively thick fragments of non-porous calcite from the ostracum of the upper valve, and a few attached valves of small radiolitids with an ostracum of non-cellular calcite escaped dissolution.

9. Discussion

In biostromes with a packed, autochthonous fabric neither shell dissolution nor larger burrows were observed. Dissolution of radiolitid shells, however, is widespread in open, bioturbated, parautochthonous rudist fabrics (Sanders, 1999). This implies a link between burrowing and shell dissolution. As discussed the burrows within the biostromes probably were produced by crustaceans. In the Holocene, burrowing by callianassids results in very high rates of sediment turnover and nutrient processing in a layer 1–3 m thick. Per square metre sea floor, the total surface of thalassinidean burrows ranges from 1 to 9 m^2; burrow volume per square metre is between 2 and 10 l (e.g. Aller and Dodge, 1974; Suchanek, 1983; Griffis and Suchanek, 1991). Most Recent burrowing shrimps feed on microbes cultivated either in the excavated sediment, and/or along the burrow walls, and/or by stuffing burrow tracts with rotting organic

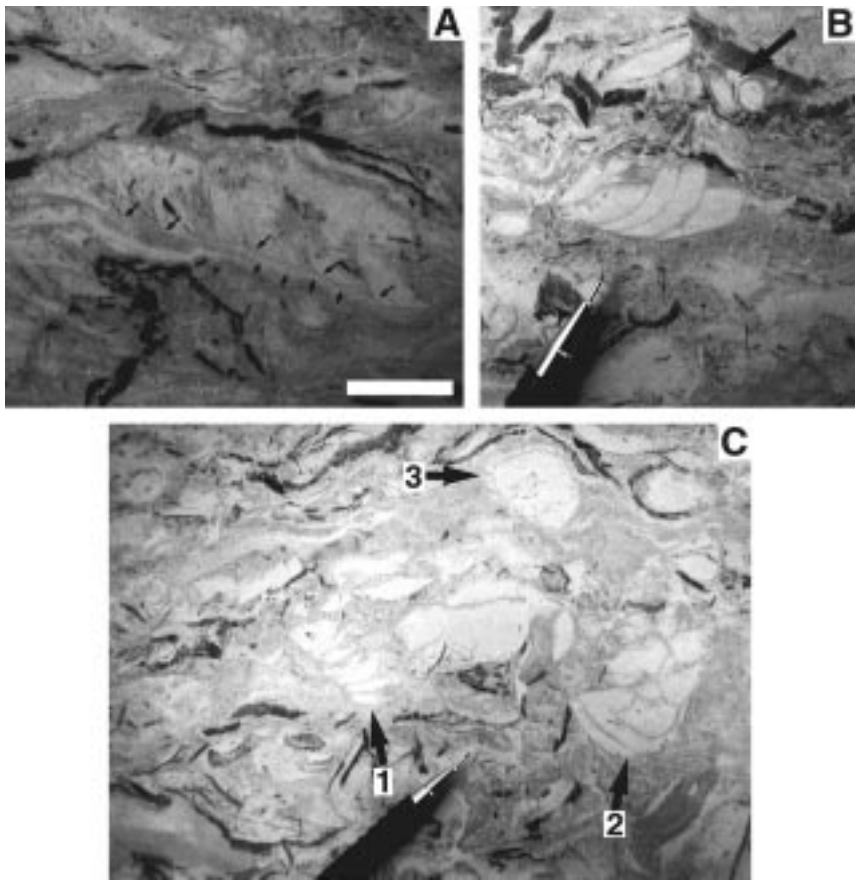

Fig. 19. Details of limestone shown in Fig. 9B. (A) Stack of crescent-shaped bodies of lime mudstone to wackestone. The lower side of the stack is a thin, well-defined layer (arrows) of lime mudstone or microsparite. From this layer, the equally thin surfaces that define the crescents branch off (branching points indicated by arrows). Scale bar: 2 cm. (B) In the centre of the photo, a short stack of crescent-shaped bodies of lime mudstone is present. Each crescent is characterized by a curved, tapering lower portion and a flat top. The crescents are laterally separated from each other by a thin, even layer of darker grey lime mudstone. The matrix is a bioclastic wackestone to packstone. In the upper part the massive (non-cellular), calcitic attached valves of two small biradiolitids (arrow) are present. Pencil is 8 mm thick. (C) Different sections through "spots" of light grey lime mudstone, showing either a more or less disintegrated array of crescent-shaped bodies (1), compaction-deformed arrays of crescents (2) or, in transversal section, a subcircular outline with a thin layer of lime mudstone along the outer surface (3). Pencil is 8 mm thick.

matter (Farrow, 1971; Braithwaite and Talbot, 1972; Tudhope and Scoffin, 1984; Griffis and Suchanek, 1991; Bromley, 1996). In bioturbated sediments, both acids (H_2CO_3, HNO_3, H_2S, H_2SO_4) and enhanced pCO_2 required for calcium carbonate dissolution are produced by oxidation of organic carbon, by sulfate reduction, denitrification from microbial metabolism, and by oxidation of solid sulfides formed during earlier sulfate reductions (Aller, 1982, 1983; Berner, 1982; Berner and Westrich, 1985; Canfield and Raiswell, 1991; Ku et al., 1999). Because of both microbial respiration and the comparatively rapid diffusion of CO_3^{2-} and HCO^-, pCO_2 is raised both within burrows and in the adjacent sediment (e.g. Pingitore, 1982; Aller, 1983), inducing acidic, reducing conditions (Ott et al., 1976). Callianassid burrowing is highly efficient in mediating calcium carbonate dissolution (compare Tudhope and Scoffin, 1984; Walter and Burton, 1990). In Holocene Fe-poor carbonate substrata, microbial sulfate reduction is followed by rapid oxidation of hydrogen sulfide, which strongly lowers pH and drives carbonate

dissolution (Boudreau, 1991). Oxygen is supplied either by biorrigation from deep-tiered burrowing, and/or from marine grass rhizomes and algae (Ku et al., 1999).

Radiolitid relicts embedded in life position indicate that in situ dissolution within the soft to firm sediment occurred (see Section 8.2.1 above). Both at Cava Romana and Cava Cortese, however, it is always the radiolitids with a boxwork ostracum that were subject to dissolution; radiolitids with a shell of massive calcite and hippuritids are preserved. Because the boxwork ostracum is built by walls a few tens of microns thick (Al-Aasm and Veizer; 1986; Pons and Vicens, 1986), dissolution most likely was related to its delicate structure (cf. Henrich and Wefer, 1986). In oxidizing diagenetic environments, the organic material within and on skeletons and tests is microbially degraded (e.g. Lewy, 1981; Canfield and Raiswell, 1991; Freiwald, 1995). The microbes are sheltered by an extracellular surface below which high pCO_2 drives carbonate dissolution (Freiwald, 1995). In Holocene tropical shallow-water carbonate environments, microalgal infestation above and within the sediment (May and Perkins, 1979) is strongly increased by both sediment turnover and enhanced microbial metabolism as a result of callianassid burrowing (Tudhope and Risk, 1985, p. 445). Annual calcium carbonate dissolution by boring microalgae amounts to at least some tens of percent of the annual sediment input (Tudhope and Risk, 1985). The large surface of the radiolitid boxwork possibly coupled with post-mortem decay of an organic coating on and within the cells, and the establishment of corrosive microenvironments by microbial infestation and boring all favoured shell dissolution and, by mechanical weakening, physical disintegration.

The presence of both emersion surfaces and dissolved rudists and, across some emersion surfaces, the "jump" in rudist preservation from relictic below to preserved above (Fig. 11) may suggest that meteoric-vadose water dissolved the shells. Taphonomic loss by in situ dissolution, however, is observed also in biostromes above emersion surfaces, whereas the rudists below the surfaces are better preserved (Fig. 7). Diagenesis of the bulk limestone probably proceeded in oxygenated, mixed marine-meteoric waters (see chapter 7). If meteoric waters were the sole dissolving agent, the typical marked differences in preservation of adjacent "boxwork radiolitids" were hardly explained. Meteoric waters probably readily entered the sediment column along the firmground burrows originally filled by winnowed bioclastic sand. Rudist relicts within these burrow fills, however, show evidence for local disintegration (slightly disoriented/disaggregated stacks to single intertabular fills floating in the grainstone). Such disintegration seems possible only if the sediment was moved subsequent to rudist dissolution, i.e. was unlithified. Locally, rudist relicts are common in which the formerly aragonitic shell parts are replaced by sediment that is of closely similar composition to and physically contiguous into the matrix (Fig. 19). Radiolitids embedded in upright position and with completely or largely dissolved shells were observed in a matrix of wackestone (Fig. 16A and B). Such an embedding seems hardly possible by meteoric-vadose dissolution even in semi-lithified sediment.

Locally, fractures filled by grainstone cut across rudist relicts, but the shell is dissolved also aside the fracture (Fig. 16C). The fractures formed comparatively late, when the limestone was sufficiently lithified for brittle deformation. Thus, although fractures most probably provided pathways for meteoric waters, shell dissolution took place earlier. For the discussed reasons, dissolution of boxwork radiolitids commenced and was completed, at least largely, within the soft to firm sediment with marine-derived pore waters.

Subsequent to dissolution in the marine sediment, during subaerial exposure dissolution by meteoric water produced the emersion surfaces. Moreover, meteoric water probably invaded the sediment column along permeable pathways, such as burrows filled by winnowed sand, existing rudist relicts, and fractures. There, meteoric dissolution overprinted the earlier features of dissolution, by corrosive widening of fractures and/or further dissolution within existing rudist relicts (Figs. 11, 16B–D and 18).

10. Taphonomic pathways

Best preservation is where a radiolitid was embedded in situ, and with the upper valve (A in Fig. 20). The intertabular space of the lower valve

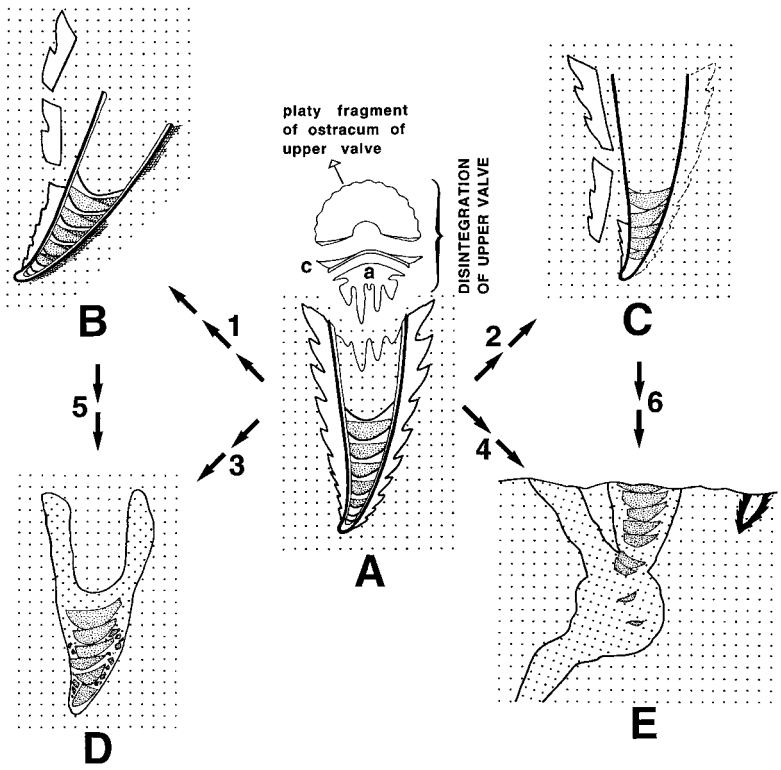

Fig. 20. Summary of radiolitid taphonomy. Intertabular fills finely stippled. Attached valve: boxwork ostracum cross-hatched, inner ostracal layer black, inner hypostracal shell layer white. Preservation A: radiolitid embedded in situ and with the free valve. The free valve, however, commonly is absent, and disintegrated into its aragonitic, hypostracal portion (a), and the calcitic, ostracal portion (c). Pathway 1, from A to B, includes disorientation of the attached valve and spalling, abrasion and dissolution of the boxwork layer. In pathway 2, from A to C, the shell is embedded upright, but the boxwork ostracum became dissolved. Pathway 3, from A to D, proceeded by shell dissolution when the matrix was firm or lithified, leaving a biomould subsequently filled with internal sediment, and containing the collapsed intertabular fills. During pathway 4, from A to E, the shell also was dissolved, or nearly so, when the sediment was riddled with firmground burrows. Later emersion may lead to truncation of all previous fabrics (shown only for type E preservation). In addition, pathways 5 and 6 were possible. Commonly, the whole range of types of preservation is observed within a single biostrome.

was filled, either partly or entirely, by internal sediment and/or by isopachous marine cement, and by blocky calcite spar. Aragonitic shell parts are preserved as blocky calcite spar. Most commonly, however, the upper valve was removed, and disintegrated into its calcitic outer layer and the aragonitic inner layer (type A preservation, Fig. 20). Upon disorientation of the lower valve and removal of the boxwork ostracum by spalling, abrasion and dissolution, a disoriented radiolitid relict resulted (type B preservation, Fig. 20). Alternatively, a radiolitid was embedded upright, but with the boxwork ostracum removed by dissolution. If, moreover, the hypostracum was dissolved, the resulting radiolitid relict (type C preservation, Fig. 20) consists of the inner ostracal layer ("calcite tube") filled with the collapsed intertabular fills. If the entire shell was dissolved, either in situ or disoriented, the biomould was filled with internal sediments, by internal breccia, and/or by calcite spar (type D preservation, Fig. 20). Where a radiolitid was next to burrows, it was completely dissolved and the intertabular fills became, either all or in part, embedded as floats within the sediment (type E preservation, Fig. 20). Finally, when a biostrome became subaerially exposed, the rudists and the burrows were truncated along an emersion surface (shown only for E in Fig. 20). Main results of the described taphonomic overprint are a

modification of both sediment texture and rudist fabric, and taphonomic loss by dissolution and fragmentation, in some cases down to the nearly complete eradication of a biostrome. Within the same biostrome, radiolitids preserved in a fashion ranging from type A to type E may be present, and are vertically/laterally closely adjacent. Moreover, intermediate stages of preservation also are common (arrows labelled 1 to 7 in Fig. 20).

In an early stage of biostrome accumulation (stage 1, Fig. 21), softground burrowing is recorded as "swirly" arrangement of bioclasts. Most radiolitids probably were preserved in type B mode. Firmground burrowers, if present, preferred deeper levels within the substrate. Dissolution of aragonite and of the boxwork ostracum probably commenced in this stage. Upon continued aggradation, because of compaction and dewatering, the deeper levels provided a firm substrate, and became riddled by "second-generation" burrows and by "third-generation" firmground burrows (stage 2, Fig. 21). In this stage, the gradients in pore fluid chemistry set up by burrowing led to dissolution of radiolitid shells, and of an unspecified amount of sediment. Deeper, abandoned tracts of the burrow network were filled with bioclastic sand. During stage 2, type B fossilization proceeded mainly by shell dissolution, whereas mechanical spalling of the boxwork ostracum became less important. Adjacent to burrows, shell dissolution led to type C and type D preservation. In sediment-filled tracts of the burrow network, in situ dissolution of shells led to type E preservation (arrows in Fig. 8). Upon subaerial exposure (stage 3, Fig. 21), an emersion surface formed on top of or closely above a biostrome, and dissolution associated with meteoric-vadose diagenesis produced radiolitid moulds.

11. Significance

Sea grasses that could act as a significant source of oxygen into bioturbated carbonate substrata (cf. Ku et al., 1999) exist since and including the Cretaceous (Den Hartog, 1970). Crustacean burrow-induced fabrics of Recent shallow-water carbonate mounds in South Florida are comparable with respect to size, geometry, fill and burrow generations to closely similar burrows in Pennsylvanian phylloid algal mounds (Tedesco and Wanless, 1995), and to the burrows described in the present paper. Shallow-marine firmground burrows exist at least since the Early Cambrian (Droser and Bottjer, 1988; Myrow, 1995). Burrowing decapods are known from the Late Devonian onwards (Schram et al., 1978). Diverse decapods, including callianassids, exist at least since the Early Jurassic (Myrow, 1995). Deep-tiered burrows of probable crustacean origin, such as *Ophiomorpha* and *Thalassinoides*, are widespread in Jurassic to Quaternary neritic rocks (e.g. Weimer and Hoyt, 1964; Hester and Pryor, 1972; Myrow, 1995; Bromley, 1996). Microborings produced by algae and/or fungi are present in shells since the Early Paleozoic (Brett and Baird, 1986). In mounds and biostromes, burrow-induced taphonomic loss by corrasion thus probably was important over large parts of Phanerozoic times. Evidence for dissolution-induced taphonomic loss should be actively searched for also in mounds and biostromes deposited in tropical shallow subtidal environments.

Deposit-feeding crustaceans produce a perpetually changing substrate surface because of sediment turnover, biodeposition by the burrowers, and reworking during high-energy events (Rhoads and Young, 1970; Aller and Dodge, 1974; Brenchley, 1981; Walter and Burton, 1990; Griffis and Suchanek, 1991). Because of sediment turnover from burrowing, the abundance each of sessile suspension-feeding epibenthos and deposit-feeding metazoans typically are inversely correlated (Rhoads and Young, 1970; Brenchley, 1981). In the Holocene, carbonate dissolution is associated with deep-tiered burrowing in muddy to sandy lagoonal substrata. Shelf margin reefs and associated bioclastics seem to suffer little or no dissolution (Ku et al., 1999). In fossil bioconstructions, thus, syndepositional carbonate dissolution may be tied to the ratio between epibenthic sessile organisms versus burrowers, to type of substrate, position on the shelf, and mean water energy. Depositional environment, sediment textures, rudist fabric and rudist preservation turn out as first-order parameters for reconstruction of the accumulation history and sediment budget of fossilized biostromes and mounds.

In view of the extensive dissolution possible, calcification rates deduced from preserved rudist shells (Steuber, 1996) not necessarily equal

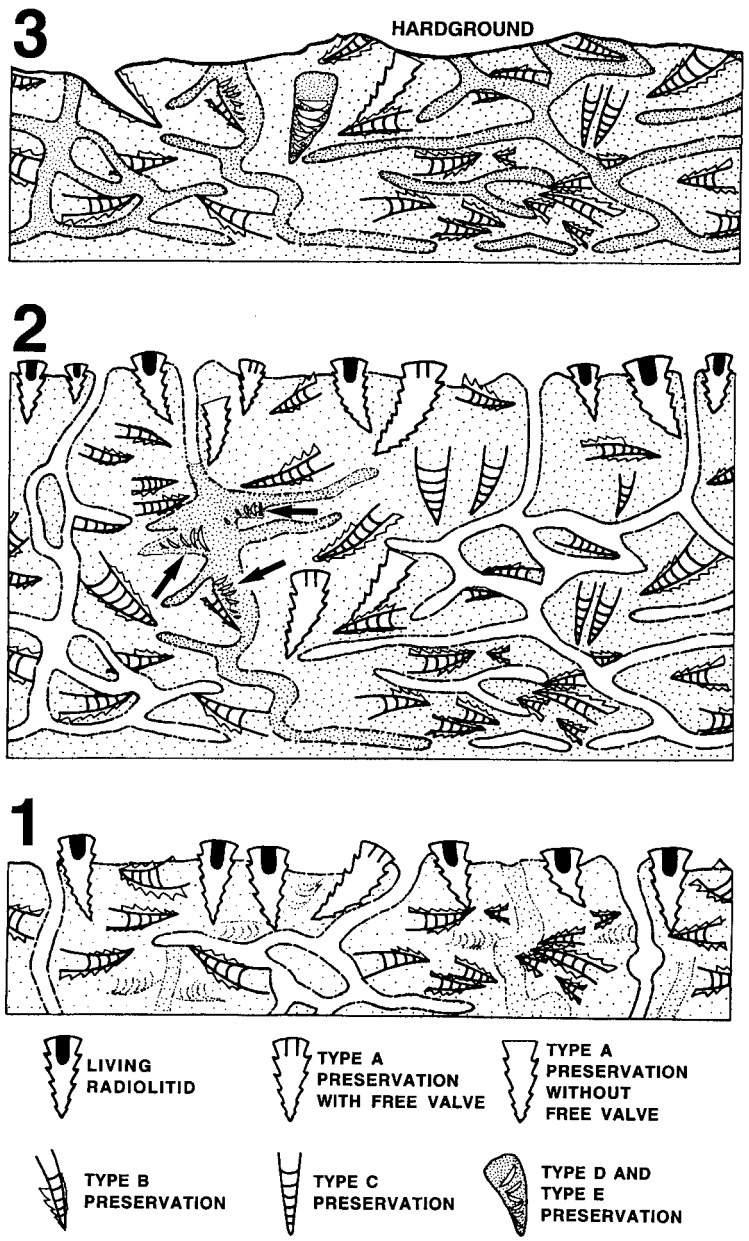

Fig. 21. Taphonomy radiolitid biostromes with an open, parautochthonous, bioturbated fabric. 1: In an early stage of biostrome accumulation, taphonomic overprint proceeded by disintegration of shells by abrasion and spalling of boxwork ostracum. Within the sediment, dissolution of the boxwork ostracum probably started. The biostrome matrix was relatively soft, and was crossed by faint, early burrows. Deep-tiered burrowers headed for deeper levels. 2: Upon continued accumulation, because of compaction, the lower and middle part of the biostrome acquired a firm consistency, thus providing a firm substrate suited for deep-tiered burrowers. In the sediment adjacent to the burrows, changed pH-conditions led to dissolution of radiolitid shells (type E preservation indicated by arrows). 3: Upon subaerial exposure, the biostrome became capped by a hardground and was subject to meteoric-vadose diagenesis. During subsequent re-submergence, the biostrome was commonly covered by bioclastic deposits (coarse stipples).

rudist-precipitated calcium carbonate available for preservation in the rock record. The amount of carbonate sediment dissolved upon burrowing of the biostrome matrix is hardly quantifiable but, by analogy to Recent carbonate environments, may have been large (cf. Walter and Burton, 1990; Ku et al., 1999). The wide variations in shell preservation, within the same biostrome and over short distances, warrant caution in interpretation. At Aurisina the patterns, variation and intensity of taphonomic loss in rudist biostromes were recognized because of the exceptional outcrop. Even in good natural outcrops the same patterns often are difficult or rarely to see. Commonly, only polished slabs and thin-sections reveal rudist relicts and emersion surfaces (see also Sanders, 1999).

12. Conclusions

In the investigated carbonate platform successions, elevator rudist biostromes with an open, parautochthonous fabric are riddled by softground to firmground burrows probably from crustaceans. During biostrome accumulation, the radiolitid fauna suffered substantial taphonomic loss by dissolution and by mechanical shell disintegration. Shell dissolution was mediated by chemical gradients in the sediment both within and near the burrows and, associated with burrowing, by enhanced microboring and microbial infestation. Dissolution was favoured by the thin-walled boxwork construction of the ostracum of the attached valve of most radiolitids. Aragonite dissolution proceeded at various stages relative to burrow excavation and filling.

Rudists with an ostracum of non-cellular calcite (hippuritids, some radiolitids) were preserved. The loss of "boxwork radiolitids" led to: (a) a substantial decrease in the number of preserved rudists, and (b) taphonomic bias towards rudists with a non-cellular ostracum. Locally, "ghost biostromes" composed of radiolitid relicts are present. Taphonomic loss by dissolution of shells and, probably, of an unspecified amount of carbonate sediment correlates with actuogeological observations by other authors that bioturbation mediates extensive carbonate dissolution, also under shallow tropical waters supersaturated with respect to calcium carbonate.

Loss of radiolitids by dissolution and fragmentation is widespread in open, parautochthonous rudist fabrics. Packed, autochthonous rudist fabrics show neither shell dissolution nor deep-tiered burrows. Although both types of rudist fabric may build biostromes, they were substantially different with respect to accumulation history, biostratinomy and early diagenesis.

In shallow-water carbonate mounds, deep-tiered burrows of probable crustacean origin were present at least since the Carboniferous. Burrow-induced fabric transformation and taphonomic loss by dissolution possibly were important over much of the Phanerozoic. Calcification rates of tropical, shallow-neritic benthic organisms can be transferred into a sediment budget available for preservation in the rock record only if dissolution in the shallow subtidal environment is considered (see also Ku et al., 1999).

Acknowledgements

The management of Cava Romana, Aurisina, and the owners of Cava Cortese are thanked for kindly allowing access to the quarries. Richard Tessadri, University of Innsbruck, is thanked for measurement of the trace elements, and for X-ray diffractometer-based determination of calcite and dolomite contents. Fritz Harald, University of Graz, guided the isotope measurements. Mauro Caffau, University of Trieste, provided a discussion on the preservation of rudists in the area of Aurisina. Lynn Walter, University of Michigan, and Franz Fürsich, University of Würzburg, provided constructive reviews.

References

Abart, R., Bojar, A.V., Fritz, H., 1998. $^{13}C/^{12}C$ and $^{18}O/^{16}O$ measurements in silicates, oxides and carbonates: a new facility at Karl-Franzens-University Graz. Mitt. Österr. Min. Ges. 143, 235–236.

Al-Aasm, I.S., Veizer, J., 1986. Diagenetic stabilisation of aragonite and low-Mg calcite. I. Trace-elements in rudists. J. Sediment. Petrol. 56, 138–152.

Allan, J.R., Matthews, R.K., 1977. Carbon and oxygen isotopes as diagenetic and stratigraphic tools: surface and subsurface data, Barbados, West Indies. Geology 5, 16–20.

Allan, J.R., Matthews, R.K., 1982. Isotope signatures associated with early meteoric diagenesis. Sedimentology 29, 797–817.

Aller, R.C., 1978. Experimental studies of changes produced by deposit feeders on pore water, sediment, and overlying water chemistry. Am. J. Sci. 278, 1185–1234.

Aller, R.C., 1982. Carbonate dissolution in nearshore terrigenous muds: the role of physical and biological reworking. J. Geol. 90, 79–95.

Aller, R.C., 1983. The importance of the diffusive permeability of animal burrow linings in determining marine sediment chemistry. J. Mar. Res. 41, 299–322.

Aller, R.C., Dodge, R.E., 1974. Animal–sediment relations in a tropical lagoon, Discovery Bay, Jamaica. J. Mar. Res. 32, 209–232.

Amico, S., 1978. Recherches sur la structure du test des Radiolitidae. Trav. Lab. Geol. Hist. Paleontol. 8, 1–131 (Université de Provence, Marseille).

Banner, J.L., Hanson, G.N., 1990. Calculation of simultaneous isotopic and trace element variations during water–rock interaction with applications to carbonate diagenesis. Geochim. Cosmochim. Acta 54, 3123–3137.

Barron, E.J., Moore, G.T., 1994. Climate model application in paleoenvironmental analysis. Soc. Econ. Paleontol. Miner., Short Course, vol. 33, 339 pp.

Bathurst, R.C., 1975. Carbonate sediments and their diagenesis. Developments in Sedimentology, vol. 12, 658 pp.

Berner, R.A., 1982. Burial of organic carbon and pyrite sulfur in the modern ocean: its geochemical and environmental significance. Am. J. Sci. 282, 451–473.

Berner, R.A., Westrich, J.T., 1985. Bioturbation and the early diagenesis of carbon and sulfur. Am. J. Sci. 285, 193–206.

Bernoulli, D., Jenkyns, H.C., 1974. Alpine, Mediterranean, and central Atlantic Mesozoic facies in relation to the Early Evolution of the Tethys. In: Dott, R.H., Jr., Shaver, R.H. (Eds.), Modern and Ancient Geosynclinal Sedimentation. Soc. Econ. Paleont. Miner. Spec. Publ., vol. 19, pp. 129–160.

Boudreau, B.P., 1991. Modelling the sulfide-oxygen reaction and associated pH gradients in porewaters. Geochim. Cosmochim. Acta 55, 1–11.

Braithwaite, C.J.R., Talbot, M.R., 1972. Crustacean burrows in the Seychelles, Indian Ocean. Palaeogeogr. Palaeoclimatol. Palaeoecol. 11, 265–285.

Brand, U., Veizer, J., 1980. Chemical diagenesis of a multicomponent carbonate system-1: trace elements. J. Sediment. Petrol. 50, 1219–1236.

Brenchley, G.A., 1981. Disturbance and community structure: an experimental study of bioturbation in marine soft-bottom environments. J. Mar. Res. 39, 767–790.

Brett, C.E., Baird, G.C., 1986. Comparative taphonomy: a key to paleoenvironmental interpretation based on fossil preservation. Palaios 1, 207–227.

Bromley, R.G., 1996. Spurenfossilien: Biologie, Taphonomie und Anwendungen. Springer, Berlin (347 pp.).

Budd, D.A., 1988. Aragonite-to-calcite transformation during freshwater diagenesis of carbonates: insights from pore-water chemistry. Geol. Soc. Am. Bull. 100, 1260–1270.

Budd, D.A., 1997. Cenozoic dolomites of carbonate islands: their attributes and origin. Earth-Sci. Rev. 42, 1–47.

Caffau, M., Plenicar, M., 1990. *Biradiolites zucchii* n. sp. nella Cava Romana di Aurisina. Geologija 33, 207–213.

Canfield, D.E., Raiswell, R., 1991. Carbonate precipitation and dissolution. Its relevance to fossil preservation. In: Allison, P.A., Briggs, D.E.G. (Eds.). Taphonomy. Releasing the Data Locked in the Fossil Record. Plenum Press, New York, pp. 411–453.

Cati, A., Sartorio, D., Venturini, S., 1987. Carbonate platforms in the subsurface of the Northern Adriatic area. Mem. Soc. Geol. It. 40, 273–288.

Cestari, R., Sartorio, D., 1995. Rudists and Facies of the Periadriatic Domain. Agip S.p.A., San Donato Milanese, 207 pp.

Colby, N.D., Boardman, M.R., 1989. Depositional evolution of a windward, high-energy lagoon, Graham's Harbor, San Salvador, Bahamas. J. Sediment. Petrol. 59, 819–834.

Cucchi, F., Pirini Radrizzani, C., Pugliese, N., 1987. The carbonate stratigraphic sequence of the Karst of Trieste (Italy). Mem. Soc. Geol. It. 40, 35–44.

Czerniakowski, L.A., Lohmann, K.C., Wilson, J.L., 1984. Closed-system marine burial diagenesis: isotopic data from the Austin Chalk and its components. Sedimentology 31, 863–877.

Davies, D.J., Powell, E.N., Stanton, R.J., 1989. Relative rates of shell dissolution and net sedimentary accumulation — a commentary: can shell beds form by the gradual accumulation of biogenic debris on the sea floor?. Lethaia 22, 207–212.

Den Hartog, C., 1970. The seagrasses of the world. North Holland, Amsterdam, 275 pp..

Droser, M.L., Bottjer, D.J., 1988. Trends in depth and extent of bioturbation in Cambrian marine environments, western United States. Geology 16, 233–236.

Ekdale, A.A., 1985. Palaeoecology of the marine endobenthos. Palaeogeogr. Palaeoclimatol. Palaeoecol. 50, 63–81.

Farrow, G.E., 1971. Back-reef and lagoonal environments of Aldabra atoll distinguished by their crustacean burrows. Symp. Zool. Soc. Lond. 28, 455–500.

Freiwald, A., 1995. Bacteria-induced carbonate degradation: a taphonomic case study of *Cibicides lobatulus* from a high-boreal carbonate setting. Palaios 10, 337–346.

Gili, E., Masse, J.-P., Skelton, P.W., 1995. Rudists as gregarious sediment dwellers, not reef-builders, on Cretaceous carbonate platforms. Palaeogeogr. Palaeoclimatol. Palaeoecol. 118, 245–267.

Goldhammer, R.K., 1997. Compaction and decompaction algorithms for sedimentary carbonates. J. Sediment. Res. 67, 26–35.

Griffis, R.B., Suchanek, T.H., 1991. A model of burrow architecture and trophic modes in thalassinidean shrimp (Decapoda: Thalassinidea). Mar. Ecol. Progr. Series 79, 171–183.

Haberman, D., Neuser, R.D., Richter, D.K., 1998. Low limit of Mn^{2+}-activated cathodoluminescence of calcite: state of the art. Sediment. Geol. 116, 13–24.

Harris, P.M., 1979. Facies anatomy and diagenesis of a bahamian ooid shoal. Sedimenta, vol. 7, 163 pp.

Harris, P.M., Kendall, C.G., St, C., Lerche, I., 1985. Carbonate cementation — a brief review. In: Schneidermann, N., Harris, P.M. (Eds.), Carbonate Cements. Soc. Econ. Paleontol. Miner. Spec. Publ., vol. 36, pp. 79–95.

Henrich, R., Wefer, G., 1986. Dissolution of biogenic carbonates: effects of skeletal structure. Mar. Geol. 71, 341–362.

Hester, N.C., Pryor, W.A., 1972. Blade-shaped crustacean burrows of Eocene age: a composite form of *Ophiomorpha*. Geol. Soc. Am. Bull. 83, 677–688.

Holland, H.D., 1978. The Chemistry of the Atmosphere and oceaNs. Wiley, New York, 351 pp.

Hudson, J.D., 1975. Carbon isotopes and limestone cement. Geology 3, 19–22.

Immenhauser, A., Schlager, W., Burns, S.J., Scott, R.W., Geel, T., Lehmann, J., Van der Gaast, S., Bolder-Schrijver, L.J.A., 1999. Late Aptian to Late Albian sea-level fluctuations constrained by geochemical and biological evidence (Nahr Umr Formation, Oman). J. Sediment. Res. 69, 434–446.

Kauffman, E.G., Johnson, C.C., 1988. The morphological and ecological evolution of Middle and Upper Cretaceous reef-building rudistids. Palaios 3, 194–216.

Kennedy, W.J., Taylor, J.D., 1968. Aragonite in rudists. Proc. Geol. Soc. Lond. 1645, 325–331.

Kidwell, S.M., Bosence, D., 1991. Taphonomy and time-averaging of marine shelly faunas. In: Allison, P.A., Briggs, D.E.G. (Eds.). Taphonomy. Releasing the Data Locked in the Fossil Record. Plenum Press, New York, pp. 115–209.

Koch, C.F., Sohl, N.F., 1983. Preservational effects in paleoecological studies: Cretaceous mollusc examples. Paleobiology 9, 26–34.

Ku, T.C.W., Walter, L.M., Coleman, M.L., Blake, R.E., Martini, A.M., 1999. Coupling between sulfur recycling and syndepositional carbonate dissolution: evidence from oxygen and sulfur isotope composition of pore water sulfate, South Florida Platform, U.S.A. Geochim. Cosmochim. Acta 63, 2529–2546.

Lasemi, Z., Sandberg, P.A., Boardman, M.R., 1990. New microtextural criterion for differentiation of compaction and early cementation in fine-grained limestones. Geology 18, 370–373.

Lewy, Z., 1981. Maceration of calcareous skeleton. Sedimentology 28, 893–895.

Lynn, D.C., Bonatti, E., 1965. Mobility of manganese in diagenesis of deep-sea sediments. Mar. Geol. 3, 457–474.

Massari, F., Grandesso, P., Stefani, C., Jobstraibizer, P.G., 1986. A small polyhistory foreland basin evolving in a context of oblique convergence: the Venetian basin (Chattian to Recent, Southern Alps, Italy). In: Allen, P.A., Homewood, P. (Eds.), Foreland Basins. Int. Assoc. Sediment. Spec. Publ., vol. 8, pp. 141–168.

May, J.A., Perkins, R.D., 1979. Endolithic infestation of carbonate substrates below the sediment–water interface. J. Sediment. Petrol. 49, 357–378.

McCrea, J.M., 1950. On the isotopic chemistry of carbonates and a paleotemperature scale. J. Chem. Phys. 18, 849–857.

Milliman, J.D., 1974. Marine Carbonates. Springer, New York, 375 pp.

Minero, C.J., 1991. Sedimentation and diagenesis along open and island-protected windward carbonate platform margins of the Cretaceous El Abra Formation, Mexico. Sediment. Geol. 71, 261–288.

Moro, A., 1997. Stratigraphy and palaeoenvironments of rudist biostromes in the Upper Cretaceous (Turonian–upper Santonian) limestones of southern Istria, Croatia. Palaeogeogr. Palaeoclimatol. Palaeoecol. 131, 113–141.

Myrow, P.M., 1995. *Thalassinoides* and the enigma of Early Paleozoic open-framework burrow systems. Palaios 10, 58–74.

Ott, J.A., Fuchs, B., Fuchs, R., Malasek, A., 1976. Observations on the biology of *Callianassa stebbingi* Borrodaille and *Upogebia litoralis* Risso and their effect upon the sediment. Senckenberg. Marit. 8, 61–79.

Peterson, C.H., 1976. Relative abundances of living and dead molluscs in two California lagoons. Lethaia 9, 137–148.

Pingitore Jr, N.E., 1982. The role of diffusion during carbonate diagenesis. J. Sediment. Petrol. 52, 27–39.

Philip, J., Babinot, J.F., Tronchetti, G., Fourcade, E., Azema, J., Guiraud, R., Bellion, Y., Ricou, L.E., Vrielynck, B., Boulin, J., Cornee, J.J., Herbin, J.P., 1993. Late Cenomanian paleoenvironments (94–92 Ma). In: Dercourt, J., Ricou, L.E., Vrielynck, B. (Eds.), Atlas Tethys: Paleoenvironmental maps. Gauthier-Villars, Paris.

Pons, J.M., Vicens, E., 1986. Nuevos datos sobre *Biradiolites chaperi* (Bivalvia: Radiolitidae) del Maastrichtiense. Rev. d'invest. Geologiques 42/43, 67–75.

Rasmussen, H.W., 1971. Echinoid and crustacean burrows and their diagenetic significance in the Maastrichtian–Danian of Stevns Klint, Denmark. Lethaia 4, 191–216.

Rhoads, D.C., Young, D.K., 1970. The influence of deposit-feeding organisms on sediment stability and community trophic structure. J. Mar. Res. 28, 150–178.

Ross, D.J., Skelton, P.W., 1993. Rudist formations of the Cretaceous: a paleoecological, sedimentological and stratigraphical review. In: Wright, P. (Ed.), Sedimentology Review, vol. 1. Blackwell, Oxford, pp. 73–91.

Sanders, D., 1996. Rudist biostromes on the margin of an isolated carbonate platform: The Upper Cretaceous of Montagna della Maiella, Italy. Eclogae Geol. Helv. 89, 845–871.

Sanders, D., 1998. Upper Cretaceous rudist formations. Proc. Fourth Meet. Austrian Paleontol. Soc. Geol. Paläontol. Mitt. Innsbruck, vol. 23, pp. 37–59.

Sanders, D., 1999. Shell disintegration and taphonomic loss in radiolitid biostromes. Lethaia 32, 101–112.

Sanders, D., Pons, J.M., 1999. Rudist formations in mixed siliciclastic-carbonate depositional environments, Upper Cretaceous, Austria: stratigraphy, sedimentology, and models of development. Palaeogeogr. Palaeoclimatol. Palaeoecol. 148, 249–284.

Sartorio, D., Tunis, G., Venturini, S., 1997. The Iudro valley section and the evolution of the northeastern margin of the Friuli Platform (Julian Prealps, NE Italy–W Slovenia). Mem. Sci. Padova 49, 163–193.

Savard, M.M., Veizer, J., Hinton, R., 1995. Cathodoluminescence at low Fe and Mn concentrations: a SIMS study of zones in natural calcites. J. Sediment. Res., A 65, 208–213.

Schram, F.R., Feldmann, R.M., Copeland, M.J., 1978. The Late Devonian Palaeopalaemonidae and the earliest decapod crustaceans. J. Paleontol. 52, 1375–1387.

Shinn, E.A., 1968. Burrowing in Recent lime sediments of Florida and the Bahamas. J. Paleontol. 42, 879–894.

Shinn, E.A., Robbin, D.M., 1983. Mechanical and chemical

compaction in fine-grained shallow-water limestones. J. Sediment. Petrol. 53, 595–618.

Skelton, P.W., 1974. Aragonitic shell structures in the rudist *Biradiolites* and some palaeobiological inferences. Géol. Méditerranéenne 1, 63–74.

Skelton, P.W., Gili, E., Vicens, E., Obrador, A., 1995. The growth fabric of gregarious rudist elevators (hippuritids) in a Santonian carbonate platform in the southern Central Pyrenees. Palaeogeogr. Palaeoclimatol. Palaeoecol. 119, 107–126.

Sribar, L., Plenicar, M., 1990. Upper Cretaceous assemblage zones in southwestern Slovenia. Geologija 33, 171–205.

Steuber, T., 1996. Stable isotope sclerochronology of rudist bivalves: growth rates and Late Cretaceous seasonality. Geology 24, 315–318.

Steuber, T., 1999. Isotopic and chemical intra-shell variations in low-Mg calcite of rudist bivalves (Mollusca — Hippuritacea): disequilibrium fractionations and late Cretaceous seasonality. Int. J. Earth Sci. 88, 551–570.

Suchanek, T.H., 1983. Control of seagrass communities and sediment distribution by *Callianassa* (Crustacea, Thalassinidea) bioturbation. J. Mar. Res. 41, 281–298.

Tarlao, A., Tentor, M., Tunis, G., Venturini, S., 1993. Evidenze di una fase tettonica nel Senoniano inferiore dell'area del Villagio del Pescatore (Trieste). Gortania 15, 23–34.

Tedesco, L.P., Wanless, H.R., 1991. Generation of sedimentary fabrics and facies by repetitive excavation and storm infilling of burrow networks, Holocene of South Florida and Caicos Platform. Palaios 6, 326–343.

Tedesco, L.P., Wanless, H.R., 1995. Growth and burrow-transformation of carbonate banks: comparison of modern skeletal banks of south Florida and Pennsylvanian phylloid banks of south-eastern Kansas, USA. In: Monty, C.L.V., Bosence, D.W.J., Bridges, P.H., Pratt, B.R. (Eds.), Carbonate Mud-Mounds. Int. Assoc. Sediment. Spec. Publ., vol. 23, pp. 495–521.

Tentor, M., Tunis, G., Venturini, S., 1994. Schema stratigrafico e tettonico del Carso Isontino. Nat. Nascosta 9, 1–32.

Tudhope, A.W., Scoffin, T.P., 1984. The effects of *Callianassa* bioturbation on the preservation potential of carbonate grains in Davies Reef Lagoon, Great Barrier Reef, Australia. J. Sediment. Petrol. 54, 1091–1096.

Tudhope, A.W., Risk, M.J., 1985. Rate of dissolution of carbonate sediments by microboring organisms, Davies Reef, Australia. J. Sediment. Petrol. 55, 440–447.

Walter, L.M., 1985. Relative reactivity of skeletal carbonates during dissolution: implications for diagenesis. In: Schneidermann, N., Harris, P.M. (Eds.), Carbonate Cements. Soc. Econ. Paleontol. Miner. Spec. Publ., vol. 36, pp. 3–16.

Walter, L.M., Morse, J.W., 1984. Reactive surface area of skeletal carbonates during dissolution: effect of grain size. J. Sediment. Petrol. 54, 1081–1090.

Walter, L.M., Burton, E.A., 1990. Dissolution of recent platform carbonate sediments in marine pore fluids. Am. J. Sci. 290, 601–643.

Wanless, H.R., 1979. Limestone response to stress: pressure solution and dolomitization. J. Sediment. Petrol. 49, 437–462.

Wanless, H.R., Tedesco, L.P., Tyrrell, K.M., 1988. Production of subtidal and surficial tempestites by hurricane Kate, Caicos Platform, British West Indies. J. Sediment. Petrol. 58, 739–750.

Weimer, R.J., Hoyt, J.H., 1964. Burrows of *Callianassa major* Say, geologic indicators of littoral and shallow neritic environments. J. Paleontol. 38, 761–767.

Wilson, J.L., 1975. Carbonate Facies in Geologic History. Springer, Berlin (471 pp.).

Woo, K.-S., Anderson, T.F., Sandberg, P.A., 1993. Diagenesis of skeletal and nonskeletal components of mid-Cretaceous limestones. J. Sediment. Petrol. 63, 18–32.